Removing Fine Solids from Bitumen through Water-assisted Flocculation using Biomolecules
Extracted from Guar Beans

By

Camila Santander

A thesis submitted in partial fulfillment of the requirements for the degree of

Master of Science
in
Chemical Engineering

Department of Chemical and Materials Engineering
University of Alberta

ABSTRACT

Non-aqueous extraction (NAE) of bitumen came to be due to the necessity for an alternative method to water-based extraction. However, NAE has its own challenges. One of the challenges is the elimination of suspended fine solids from solvent-diluted bitumen. This research focuses on the effect of natural settling additives in the sedimentation of the fine solids and how the alteration of the aromatic character of the solvent affects the performance of such additives. In order to find out if the additives could aid in settling we destabilize bitumen-coated silica particles in toluene with the addition of water and biomolecules extracted from Cyamopsiste tragonolobuosr L. Taup., i.e., high and low molecular weight guar gum (HGG and LGG), respectively. Lastly, water and water diluted HGG were added to an array of non-treated bitumen-solvent (toluene, cyclohexane and their mixtures) slurries, to interact with fine solids and promote settling. With sedimentation tests and focused beam reflectance measurement (FBRM) analysis, we demonstrate that these biomolecules can facilitate the settling of the solid particles in toluene although the underlying mechanisms differ between these two biomolecule cases. FBRM was also used in testing the effects of aromaticity. When toluene-cyclohexane mixtures are introduced, the overall solid content is reduced, measured with standardized protocols such us ashing and hot filtration. To complement the results found in the aromatic related tests, the effect of temperature and solvent to bitumen ratio where studied. Due to high viscosity of bitumen diluted slurry, the increase in temperature is suggested to further improve the dispersion of HGG and, therefore, increase settling rates This study attempts provide alternative solutions to fine solids removal without using synthetic additives or affecting bitumen extraction and recovery from NAE process.

This thesis is an original work by Camila Santander conducted at the University of Alberta, North campus. All projects and associated methods were approved by the University of Alberta Research Ethics Board, Project Name "Removal of hydrophobic bitumen-coated fine solids from NAE bitumen using water droplets with modified interfacial chemistry and bio-inspired polymers" developed by the Institute for Oil Sands Innovation. A version of Chapter 4.1 has been accepted for publishing in the Petroleum Science journal under the title of "Destabilization of Bitumen-coated Fine Solids in Oil through Water-assisted Flocculation using Biomolecules Extracted from Guar Beans".

I was the lead investigator, responsible for all major areas of concept formation, data collection and analysis, as well as manuscript composition. Jing Liu was involved contribution of chapter 4.1 manuscript. Dr Xiaoli Tan and Dr Qi Liu was involved throughout the project in concept formation and manuscript composition. Dr Hongbo Zeng was the supervisory author on this project.

ACKNOWLEDGEMENT

TABLE OF CONTENTS

TABLE OF FIGURES

LIST OF TABLES

CHAPTER 1   INTRODUCTION

1.1 Oil Sands

Canada holds the third largest proven oil reserve in the world, after Venezuela and Saudi Arabia, as oil sands. According to the Alberta Energy and Utilities Board (AEUB), the reserves of oil sands are over 174 billion barrels, the crude bitumen production was 2.83 million bbl/d in 2017 and the oil sands deposit occupy a total area of 149,000 square kilometers in the Athabasca basin of north-eastern Alberta and Saskatchewan.[1] Oil sands are primarily, a mixture of bitumen, sands, clays and salty water. The primary value in this mixture is high molar mass petroleum known as bitumen, characterized by significantly high viscosities, high densities, relatively high heavy metal concentrations, however, a low ratio of hydrogen to carbon in comparison with conventional oil.[2] By analyzing the composition of the hydrocarbon extracted i.e., concentration of saturates, aromatics, resins and asphaltenes; the type of bitumen is determined.[3]

1.2 Bitumen Extraction

Depending on the depth of the deposit, there are two ways to recover oil sands. If the deposit is near the surface, the oil sands are recovered by open-pit mining, if not (below 70 m from the surface) the *in-situ* drilling method has been found more suitable.

The *in-situ* drilling method consists in injecting steam and/or solvents into the underground wells previously drilled. In consequence, the temperature rises, and the bitumen becomes less viscous, allowing it be pumped to the surface.[4,5]

A model plant to extract bitumen using hot water was established by Dr. Clark in 1929, and by 1969, the hot water extraction (HWE) process was commercially applied for shallow oil sands deposits. With the assumption that the surface of mineral matters is surrounded by a thin

film of connate water,[6] steam is injected into the ore in order to facilitate the release bitumen.[6,7] The bitumen extracted is then transported to flotation beds, where the bitumen is separated from the sand by agitation and air injection. The sand settles in the bottom and due to buoyancy effect, the bitumen is collected by the bubbles of air creating an oil-rich froth that overflows at the top of the vessel.[4] This froth contains approximately 60 wt.% bitumen, 30 wt.% water and 10 wt.% solids, which must be processed further to eliminate the unwanted water and solids from bitumen, known as froth treatment. After froth treatment, the bitumen content is usually more than 99% by weight, therefore, ready to be sent to upgrading units. For the time being, the majority of raw bitumen in Alberta is produced by mining the ore, followed by a water-based extraction process.[8] Over 80% of the bitumen extraction is done by in-situ mining.

In Hot Water Extraction (HWE), water-in-oil or oil-in-water emulsions are present throughout the process, especially in the bitumen froth and in the tailings (waste from the process). The water droplets in the water-in-oil emulsions contain dissolved salts that lead to equipment corrosion in upgrading processes. The oil droplets in inverse emulsions reduce the recovery of bitumen and cause many difficulties in dealing with wastewater. Thus, the coalescence of water/oil droplets is mandatory, however, challenging.

In addition, high consumption of fresh water as well as fast accumulation of toxic and slow-setting mature fine tailings appear as a result of HWE bitumen processing. Even though the current commercial HWE processes can recycle a large portion of process water (~ 80%), importation of additional barrels of fresh water from rivers (i.e., make-up water) are still required to produce each barrel of bitumen. On average, 3.5 barrels of fresh water are required to produce 1 barrel of bitumen.[9]

1.3 Asphaltenes and Asphaltene model compounds

Asphaltenes are one class of compounds present in crude oil defined not by their structure but their solubility class. They are commonly defined as soluble in toluene but insoluble in short-chained hydrocarbons such as heptane or hexane.[10,11] Asphaltenes are of amphiphilic nature, and they can absorb water-oil interface like surfactants, with the polar groups residing in aqueous phase and non-polar group in oil phase.[12] Some research work found that non-swelling clay minerals such as kaolinite, illite and chlorite, retain organic residue in the form of patches on the outer surface of the minerals, whereas swelling clay minerals like smectite and montmorillonite, are able retain organic residue in their interlayer space.[13] It was demonstrated that the presence of the connate water layer on the mineral surface reduces the adsorption of organic residues to some degree.[14–17]

1.4 Importance of research

Water-based bitumen extraction keeps raising environmental concerns due to the alarming amount of water used in the process, as well as the increasing size and number of tailings ponds threatening the ecosystem. In addition, Canada's largest growing source of greenhouse gas is the oil sands industry, contributing a third of the country's emissions. This greenhouse gas surplus is attributed to the high amount of energy needed to heat the water, as mentioned in the Bitumen extraction section.[18] These environmental red flags lead industry and academia to find alternatives to make oil sands processing a more sustainable industry.

One of the alternatives to this process is the non-aqueous method of bitumen extraction, involving organic solvents that in theory can be recycled and reused during the process. However, the presence of fine solids in the bitumen hinders the sustainability of this extraction

method. The nanoscale fine solids are covered in bitumen and, therefore, are stable in the organic medium, rendering them difficult to remove. A detailed description of the process is presented in a further section (Section 2.3).

Our research focuses on grounding non-aqueous extraction as a viable method for bitumen recovery by presenting an environmentally friendly and effective alternative to remove fine solids from the extracted bitumen.

1.5 Objectives of this research

The objective of this thesis is to focus on using biodegradable molecules, in addition to water, to enhance effectively the sedimentation and removal of fine solids hailed from non-aqueous extracted bitumen, specifically biomolecules extracted from the plant (*Cyamopsiste tragonolobuosr L. Taup*) also known as Guar gum. More specific objectives are:

- To measure and compare the settling rate and turbidity of bitumen coated silica in toluene, with the addition of DI water, low molecular weight Guar gum (LGG), high molecular weight Guar gum (HGG) and both gums in aqueous solutions.

- To monitor the formation of bitumen-coated silica aggregates in toluene assisted by DI water, low molecular weight Guar gum (LGG), high molecular weight Guar gum (HGG) and both gums in aqueous solution.

- To monitor the formation of fine solids aggregates from Athabasca bitumen (containing ~ 0.6 wt% solids) provided by Syncrude Canada Ltd in toluene assisted by DI water and HGG.

- To investigate the effect of modifying the aromatic character of solvents in the bitumen-solvent system (i.e., toluene, cyclohexane and their mixtures) on the

aggregation of fine solids from Athabasca bitumen (containing ~ 0.66 wt% solids) provided by Syncrude Canada Ltd assisted by DI water and HGG.

- To determine the residual solid content of bitumen-solvent system treated by DI water and HGG.

- To study the effect of industrial operation parameters such as resident time and temperature, in solid content results from DI water and HGG treated bitumen-solvent slurry.

1.6 Thesis Structure

The thesis is developed through 5 chapters. In chapter 2, the background information, on which this project was based, is presented. Chapter 3 introduces the methodologies applied in the experiments of this research. In chapter 4, the results are provided and discussed. At last, in chapter 5, the conclusions from this research and suggestions on future studies are provided.

CHAPTER 2   LITERATURE REVIEW

2.1 Bitumen composition and rheology

Most oil sands ores consist of bitumen, water, sand and clays (or fine solids). The deposits in Athabasca, from which the oil industry in Canada relies on, approximately contain 82-85% of mineral solids.

Bitumen is composed of 83.2% of Carbon, 10.4% of Hydrogen, 0.94% of oxygen and 4.8% of sulphur.[12] Bitumen is a mixture of organic compounds such as linear aliphatic, cycloaliphatic and aromatic. Linear aliphatic compounds are saturated linear carbon compounds (e.g., n-heptane). Cycloaliphatic compounds are ring structures that are composed of saturated carbon atoms (e.g., cyclohexane), or cyclic structures that have a low number of unsaturated groups (e.g., cyclohexene), and aromatic compounds are those compounds that have at least one aromatic ring (e.g., benzene). The wide range of compounds and a varying nature of these compounds from bitumen to bitumen, in addition to the interaction between molecules and the dilution effect of other molecules in the mixture are reflected in the properties of bitumen.[19,20] Several metallic elements are, also, present in bitumen such as sodium, vanadium, iron, nickel and chromium.[20]

Asphaltenes and maltenes are the two main bitumen groups. The maltenes are further subdivided into saturates, aromatics and resins. This classification is useful since it enables the rheological analysis of bitumen against broad chemical composition.

The rheological behavior of bitumen can be classified according to the temperature of the process: linear elastic regime at low temperature, viscous regime at high temperature and viscoelastic regime at intermediate temperature.

The linear elasticity is achieved at temperatures below 25°C and short loading times (high frequencies),[21] where the bitumen behaves as an elastic solid. The linearity in the viscous regime is achieved at temperature above 60°C and long loading times (low frequencies), where the material behaves almost entirely as a Newtonian fluid. The non-linear behavior is found in the viscoelastic regime in moderate temperatures (25-60°C) and moderate loading times.[22,23] This moderate range of temperatures correspond to the temperature conditions used in the practical operation and will be studied as part of this research.

2.2 Asphaltenes

Asphaltene constituents have the highest molecular weight and most polar constituents in crude oil. They are dark brown to black friable solids without definite melting point and usually foam and swell on heating to leave a carbonaceous residue.[24] The amount and the characteristics of the asphaltene constituents in crude oil depend on the source of the crude oil. During petroleum refining, the asphaltene constituents are non-distillable and remain in the residual fuels (the lowest-value petroleum products from a refinery) as the distillable fractions are removed.[25] The amount of carbon and hydrogen in asphaltenes vary usually over a narrow range, corresponding to a hydrogen-to-carbon ratio of $1.15 \pm 0.5\%$. It is the heteroatom content that the asphaltenes differ significantly from the crude oil source. Asphaltenes contain amounts of nitrogen, oxygen, sulphur and trace amounts of nickel and vanadium. But usually the amount of oxygen and sulphur can vary from 0.3 to 4.9% and 0.3 to 10.3%, respectively.[26,27]

They are obtained from petroleum by the addition of a nonpolar solvent (hydrocarbons) with a surface tension lower than that of 25 dyne cm^{-1} at 25C (n-pentane, iso-pentane and n-heptane). Asphaltene constituents are soluble in liquids with a surface tension above 25 dyne cm^{-1}, like pyridine, carbon disulfide, carbon tetrachloride, and benzene, however, insoluble in

liquefied petroleum gases, such as methane, ethane, and propane. The oil fraction is composed of saturates and aromatics, therefore, soluble in n-pentane or in n-heptane.[24,25]

2.2.1 Clay minerals

The coating of bitumen components modifies the properties of clay minerals, both physically and chemically, causing significantly different behaviors. Therefore, even though, most clay minerals are naturally hydrophilic, their surface wettability is altered to become hydrophobic by the adsorption of hydrocarbons such as asphaltenes, resins, or humic materials.[28,29] Such modification affects the particle separation, since the wettability of the fine particles determines the behavior and tendency to follow the aqueous or organic phase, including the interface.[30,31] In addition, a thin layer of water was proposed to exist on the surface of the minerals, trapped between the bitumen coating and the mineral. This aqueous film, known as a connate water layer, is formed and stabilized due to the electrostatic forces hailing from the electrical double layer at the oil/water interface and water/sand grain interface.[32,33] It has also been suggested that only a fraction of the total water are present as films, the rest are found in the form of pendular rings in the grain to grain contact area.[33–35]

The interaction forces for aggregation of petroleum asphaltenes were proposed by Gray et al.[36] in the form of supramolecular assembly model which includes hydrogen bonding, acid−base interactions and metal coordination complexes among others. The nature and content of heteroatoms (such as N, O, and S) in the organic molecules influence the asphaltene adsorption onto mineral solid surfaces, due to the formation of hydrogen bonds. In addition, polar-polar interactions have been found in the bitumen covered mineral surfaces. Carboxyl groups were found to be among the common and effective chemical species that bound the organics and minerals together, additionally to cations (Ca^{2+}) that bind at oil−mineral interfaces and bridge

them. It was also suggested that organic matter could be physically entangled with surfaces of the mineral solids.[30,37,38]

Particle size, surface area and cation exchange capacity, are properties that affect bitumen adsorption. When the size is in the smaller range, cation exchange capacity and specific surface area have been found higher, therefore, a stronger capability of adsorbing bitumen organic matter. Unfortunately, the understanding of the bitumen adsorption on specific types of clays, such as swelling and non-swelling is still an on-going process.[30]

The uniformity of the bituminous layer on the clay's surface has been studied, providing strong evidence of a non-uniform layer, on the contrary, it was found that even at high adsorption densities the bitumen coating is in form of patches.[30,31,39] Due to this "patchy" surface, the clay minerals have two distinct faces: a hydrophilic and hydrophobic one. Depending on the fraction coated with bitumen the domain is defined, for instance, with a large portion of the particle coated with bitumen, the hydrophobic character is predominant. Such a surface configuration renders the clay particles bi-wet, therefore has a tendency to concentrate at oil/water interfaces.[40]

2.3 Non-Aqueous extraction (NAE)

Bitumen extraction from oil sands using organic solvents instead of water offers the potential to eliminate tailing ponds and improve energy efficiency. The earliest approach to an extraction with low water content was using naphtha as the solvent and used a small amount of water to bind the fine solids. Bitumen recovery was over 95% using a solvent mixture that contained 87% naphtha and 13% water. Later, benzene, toluene and kerosene replaced naphtha, obtaining higher mass transfer rates when high aromaticity was involved. Even though there was high recovery of bitumen, solvent recapture from the extraction gangue presented its challenges,

high-boiling-point solvents reduces the solvent recovery from large volumes of sand. [9,41]

In organic solvents, a considerable number of fine solids migrate to the mixture of bitumen and solvent during the NAE process, consequently the bitumen extracted cannot go through downstream operations.[42] Size and hydrophobicity of the fine solids limit conventional separation methods such as gravitational or centrifugal settling followed by filtration from being effective.

In the nonaqueous extraction (NAE) process, an organic solvent is used to solubilize bitumen from the sand grains trapping it. The solvent selection is key for NAE to be successful, physical properties, such as boiling point, density, viscosity and solvation power, specially the latter which characterizes the overall dissolving capability of a solvent and measures the capacity of mixing in any ratio without separation of two phases miscible liquids of liquid materials, will help determine the optimal solvent and solvent ratio.[43] However, the selection of the optimal solvent is very challenging due to several contradictions between the processes in which the solvent is involved. Bitumen recovery increases with the aromatic character of the solvent.[44] Solvent blends with aromatic compounds appear to have better extraction performance than its solvents. For hydrocarbons having the same number of carbon atoms, often an aromatic solvent possesses the highest boiling temperature, followed by cycloalkane and alkane. However, in the following process, of solid settling and solvent recovery, alkanes and cycloalkanes generally show better performances, specially the former.[43,45]

2.4 Guar gum

To target the clays' hydrophilic patches, water and other hydrophilic and amphiphilic compounds (polymers) have been suggested to accelerate the aggregation and further settling

process of the fine solids.[46] However, even with high settling rates, separation between such compounds and the fine solids presents its challenges itself, including the costs of production of the specific compound.

Polysaccharides are complex chain of monosaccharides units interlinked with glycosidic linkages. Natural polysaccharides are non-toxic, safe, biodegradable, biocompatible, renewable and cost-effective and readily available. Most of the natural polysaccharides are used in food, pharmaceutical and cosmetic industries due to their non-toxicity and safety for humans. However, the applications of these large and heavy molecules have increased; thickener, suspending agent, moisturizer, emulsifier, emollient as well as wound-healing agents. This gum is capable of producing considerable increase in the viscosity of solution, even at smaller concentrations.[47]

Natural gums are polysaccharides capable of producing considerable increase in the viscosity of solution at small concentrations. They are generally insoluble in oils or organic solvents such as, hydrocarbons, ether or alcohols, however, a few have been found to have amphiphilic behavior. On hydrolysis, they may yield combination of arabinose, galactose, xylose, rhamnose, dextrose, mannose, uronic acids, etc. Depending upon the source, they are classified as plant exudate gum, seed gum, microbial gum or marine gums. Seed gums, such as **guar gum**, tamarind gum, locust bean gum, etc., are obtained from the embryos of seeds, where they are stored as food reserve.[47,48]

Guar gum being readily available at cheaper cost is extensively investigated by various researchers. It consists of linear backbone chains of $(1 \rightarrow 4)$-β-d-mannopyranosyl units with branch points of α-d-galactopyranosyl units attached by $(1 \rightarrow 6)$ linkages. The absence of any uronic acid, makes guar gum different from the great majority of plant gums and mucilages.

Guar has got one of the highest molecular weight (10^6) of all naturally occurring water soluble polysaccharide.[48] Aside from the polysaccharide, another Guar gum is found in the industry i.e., disodium[[[5-(6-aminopurin-9-yl)-3-hydroxyoxolan-2-yl]methoxy-hydroxyphosphoryl]oxy-oxidophosphoryl] hydrogen phosphate with low molecular weight both of which are extracted from the same plant (*Cyamopsiste tragonolobuosr L. Taup*). For simplicity, LGG and HGG will be used to distinguish these two polymers. Both have been recently used in water treatment and mining.[49–52] Figure 1 shows the chemical structures of these two gums. LGG has a hydrophilic phosphate group and it behaves completely ionic in water. On the other hand, the HGG is a kind of galactomannan, showing a hydrophilic nature due to the numerous hydroxyl groups across the chain.
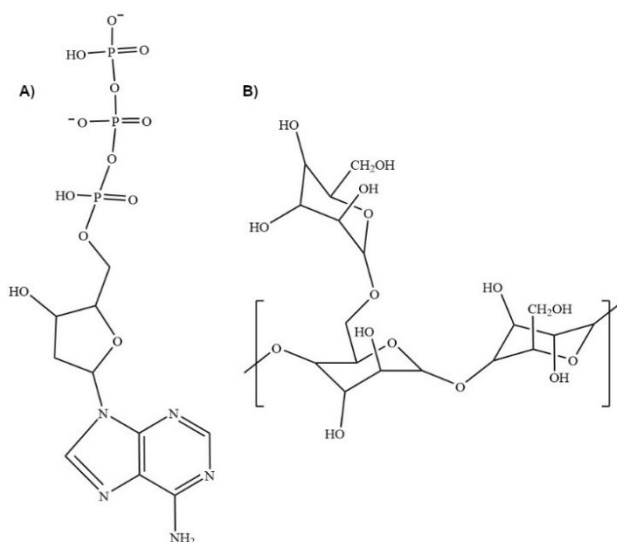
Figure 1 Guar gum structures. A) low molecular weight (LGG) guar gum and B) high molecular weight (HGG) guar gum[49,53]

2.5 Aggregate formation

Aggregate formation of fine solids induced by Guar gum is what this research aims for. The stability of suspended fine solids is significantly influenced by the collision frequency, and

any aggregates formed upon external stimulus (e.g., additives) will in turn impact the collision frequency. During the flocculation or aggregation process, floc aggregation and breakage occur at the same time suggesting that both the breakage rate parameters and the collision efficiencies would change under different flocculant concentrations.[54] The rate of flocculation depends, as well, on other factors, such as the magnitude of the attractive force, the hydrodynamic interactions between particles, and the polydispersity of the system.[55]

2.5.1 Collision Theory

The collisions between particles can facilitate and lead to the formation of aggregates. Three phenomena explain the cause, effect and frequency of collisions. First, Brownian motion, defined as the random movement of colloidal particles in a fluid, this random movement can bring two particles together through diffusion. The second phenomenon, velocity gradient, hails from fluid motion (mixing, sonicating, in flow, etc.), causing particles, depending on the size, to collide with each other due to the new velocity gain through the motion. And third, the differential settling, this phenomenon is induced when larger aggregates are formed and start to settle, when settling occurs the motion caused by it, leads to smaller aggregates or adjacent particles to collide.
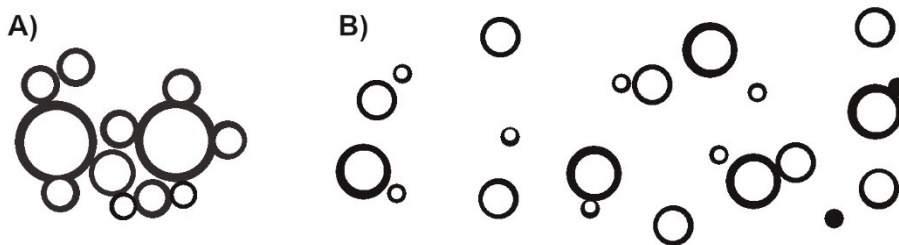
Figure 2. Illustration of fine solids suspended in A) aqueous solution and B) in organic solvent

However, depending on the fluid medium and the characteristics of the solids,

flocculation and formation of aggregates happens differently. In aqueous media, fine solids could aggregate naturally after being mixed due to collisions because of their hydrophobic patches. However, in an organic solvent due to the predominant factor of the bitumen coverage on the surface of the clays, fine solid are stable without forming aggregates, as shown in Figure 2. Mixing might induce binding; however, flocculants or binding aids accelerate the process and optimize formation of stronger aggregates.

Mixing promotes the aggregate formation by enhancing the collision rates between particles and binding molecules. Therefore, as previously mentioned, aggregate formation is governed by two events: 1) aggregation due to contact of particles and 2) fragmentation (breakage) (Figure 3).[56][57]
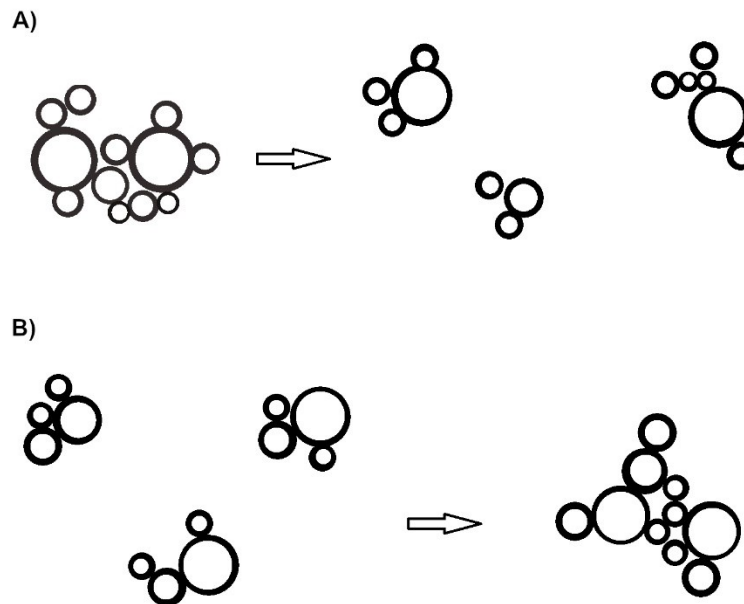
Figure 3 Diagram of the effect collisions on aggregate formation and breakdown: A) An aggregate breaks into smaller sections or particles due to high shear rate; B) Flocculation of smaller flocs or particles by the increased collision forces and probability of collision.

Aggregate formation increases the particle size from submicroscopic particle or micro-aggregate to visible suspended particles. Aggregate size continues to build with additional collisions and interaction with added binding aids (polymers, flocculants or inorganic coagulants). Macro-aggregates are formed and high molecular weight molecules, called binding aids, may be added to help bridge, bind, and strengthen the floc, add weight, and increase settling rate, as shown in Figure 4. To prevent aggregate from tearing apart or shearing, the mixing velocity and energy are usually tapered off as the size of the aggregates increases. Once the aggregates are torn apart, it is difficult to get them to reform to their optimum size and strength.
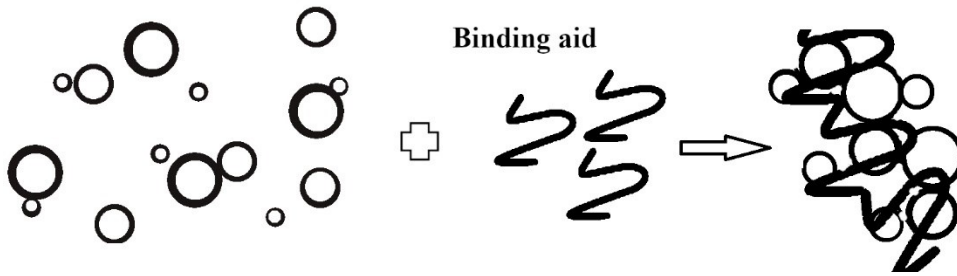
Figure 4 Diagram of the effect of a binding aid introduced during the formation of aggregates.

In addition, some studies suggest that the most efficient collisions between the binding aid and the suspended particles occurs at the optimal dosage of the former.[56,58] This optimal dosage depends on charge neutralization and bridging mechanism, however, the binding mechanism plays a key role for producing larger and stronger floc size.[58]

2.5.2 Attractive forces in organic media

As collisions happen, the particles experience attractive and/or repulsive forces among them. These forces affect the aggregation process: by modifying the collision efficiency and the strength of the aggregates formed. The alteration of collision efficiency is explained when there is strong repulsion between particles, the collision does not keep the colliding particles together,

and therefore, the aggregate does not form. On the other hand, strength of the aggregates whether the aggregates would break up under hydrodynamic shear forces. In non-aqueous media; steric repulsion, cross bridging and van der Waals attraction are the forces that determine the behavior and formation of aggregates.

2.5.2.1 Steric repulsion.

The adsorption of bitumen onto the surfaces of suspended solids can significantly affect particle-particle interactions. When two particles with covered surfaces approach one another, it will cause the brushes to repel one another. These brushes are the extension of the bitumen coverage, because of the solvent used. In "good solvents", the bitumen in the surface is also dissolved in the solvent, therefore, the bitumen extends in a brush like formation around the particle; in "poor solvents" the brushes are not strong enough, thus making it possible for van der Waals attraction to overcome barriers and result in aggregation. Such barrier is known as steric repulsion.

2.5.2.2 Cross bridging

When adding molecules to aid the formation of aggregates there are two options to choose from depending on the concentration; a molecule big enough to fully cover the particle's surface and a smaller molecule, however, long and flexible to bridge between two particles (if the distance between particles is comparable to the size of the bridging molecule). The latter provides a link between two particles nearby and is known as cross bridging.[59] In this study, we use large molecules as an additive.

2.5.2.3 van der Waals attraction forces

The universal attractive force between any two-point particles, such as atoms and molecules, is known as the van der Waals force. It consists on the sum of three different types of dipole-dipole interactions: Permanent dipole (Keesom forces), Induced dipole (Debye forces) and Induced dipole (London dispersion forces). This force is always attractive; however, the magnitude depends on the particles size, the distance between them, and the composition of the particles.[60]

2.6 Experimental methodologies

2.6.1 Settling rate measurement

The rate at which the solids are settling is done by tracking the interface position is tracked during settling by visual observation. When bitumen solutions of high concentrations are used, the visibility is low, the motion of the interface cannot be followed easily, and the method becomes ineffective. However, for the present work, focused beam reflectance measurement (FBRM) was used to monitor the settling process and determine the settling rate, which has been designed to work in opaque systems.
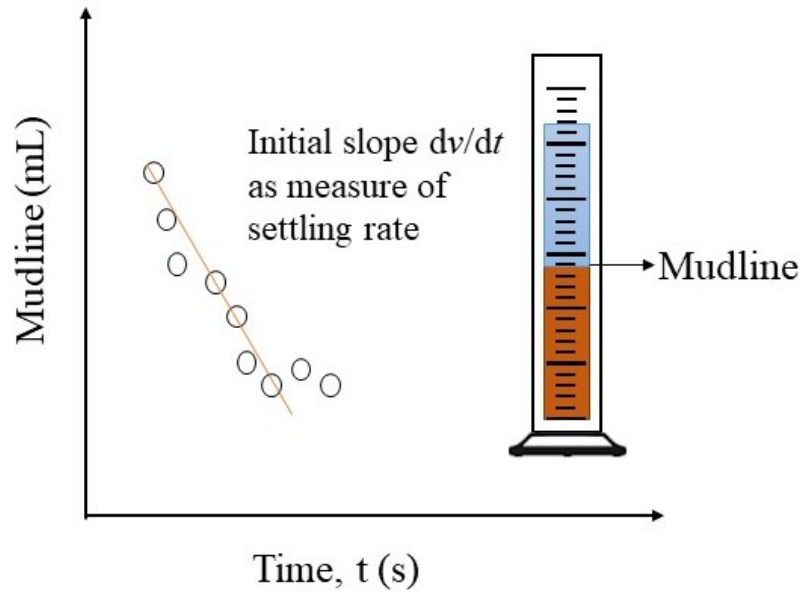
Figure 5 Typical plot of the movement of the mudline with time in a settling process.

2.6.2 Aggregate formation and size tracking

To track the size of colliding fine solids and additives during a settling process, focused beam reflectance measurement (FBRM) size analyzer was applied in this work. FBRM has been a powerful technique that follows the size distribution of particles, which can provide the information of particle count and chord length (linear size) in real time. Barret and Glennon explained the working principle of FBRM and demonstrated its potential of monitoring particle size distribution in a multi-particulate and agitated suspension.[61] The use of FBRM can also help monitor the aggregation process of fine solids and enable process control and optimization.[62]
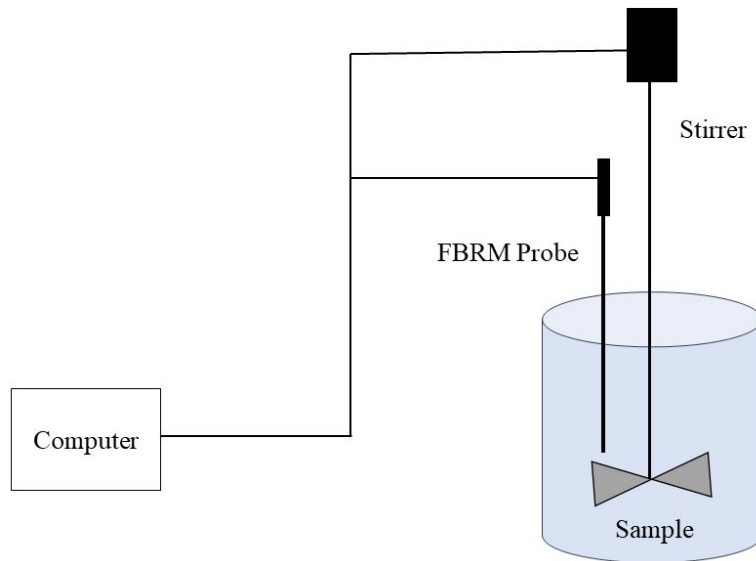
Figure 6 Focus Beam reflectance measurement (FBRM) set up

2.6.3 Solid content determination

In order to quantify the solids left in the supernatant, after settling is done, there are two industrially used standardized tests that were performed for this project: ashing and hot filtration. The selection of either of the methods depends on the expected solid content; ashing is initially performed to predict if the solid content is above or below 0.2wt%, and for confirmation of solid content below 0.2wt%, hot filtration should be test done.

2.6.3.1 Ashing

This test method determines ash content in distillate and residual fuels, gas turbine fuels, crude oils and other petroleum products. Ash presence is considered to be undesirable impurities or contaminants, also known as mineral particles or fine solids. This technique is usually performed by placing the sample in an open inert vessel know as crucible and destroying the combustible (organic) portion of the sample by thermal decomposition using a muffle furnace. The objective of this procedure is to burn the additional content surrounding the fine solids, such

us bitumen, solvent and all organic matter, leaving the fine solids (inorganic content) to form ashes when heating at 775ºC. A drawback of this technique (fixed or variable pipette techniques) is that it is time consuming (up till 24 hrs all together) and sensitive to operator skills.[63]

2.6.3.2 Hot Filtration

This test method determines the sediment in crude oils by membrane filtration. Sometimes during a gravity filtration, solids will accumulate in the filter funnel and may block the funnel, stopping filtration. Or in this research case, the surface of our particles is covered by a layer of bitumen that can cause the solids to stick to the filtration equipment. This problem can be avoided by using hot filtration where the whole filtration apparatus is heated in order to prevent the solution from cooling significantly and some of the organic matter to evaporate. A representative fraction of a crude oil sample or an oil derived sample is dissolved in hot toluene to be further filtered under vacuum through a 0.45 μm porosity membrane filter. The filter with residue is washed, dried, and weighed to give the final result.[64]

CHAPTER 3   MATERIALS AND EXPERIMENTAL TECHNIQUES

3.1 Materials and equipment

Silica particles with diameter of ~ 0.5-10 μm (Sigma-Aldrich) were used as the model fine solids in the first tests. Athabasca bitumen (~ 0.6 wt% solids) provided by Syncrude Canada Ltd was used. HPLC grade toluene and cyclohexane (certified ACS grade, > 99%) from Fisher Scientific were used as the organic solvents to disperse the bitumen and study. LGG ($C_{10}H_{14}N_5Na_2O_{12}P_3$, Mn ~ 6K, Fisher Scientific) and HGG (Mn ~ 500K, Everland, Natural Canadian products) were used as the additives in the sedimentation tests. Milli-Q water (Millipore deionized with a resistance of ≥18.2 MΩ·cm) was used as the water additive in the sedimentation tests. For solid content determination nylon Whatman membrane filters (pore size 0.45 μm and diam. 47 mm) were used.

Focused beam reflectance measurement (FBRM G400, Mettler Toledo, USA) size analyzer was used in this work. The measurement range is 0.5-2000μm.[61,65]

3.2 Preparation of bitumen-coated silica particles

For controlled sedimentation tests, bitumen-coated silica particles were prepared to mimic the indigenous fine solids in NAE bitumen. Bitumen was first diluted with toluene and centrifuged at 8964 rpm (9000 RCF) for 1 h to eliminate the trace number of solids (~ 0.6 wt%) contained in bitumen, after which toluene was removed from the bitumen via evaporation in vacuum. The treated bitumen was then dissolved in toluene again to prepare the bitumen-in-toluene solution (0.2 wt%) and the solution was mixed in the ultrasonic bath for 10 min. Then, clean silica particles were mixed with the bitumen-in-toluene solution at bitumen/silica mass ratio 1:5 (1B5S). The mixture was sonicated for 5 min to separate any solid aggregates, agitated

for 10 min using a magnetic stirrer (1000 rpm) and thoroughly washed with toluene through centrifugation (6000 rpm) for multiple times until the supernatant was clear. The resultant particles were then recovered and dried in a fume hood for 8 h. Such bitumen-coated silica particles have a new-found diameter ranging between ~ 1 and 5 μm, as demonstrated by FBRM (Appendix A).

3.3 Preparation of additives

Apart from water, all additives were prepared. To facilitate the mixture between LGG and HGG in the slurry, a dilution of each gum in toluene at~90 wt% is done. For LGG and HGG aqueous, guar gum was first dissolved in water at a concentration of 200 mg/L.

3.4 Sedimentation tests for bitumen-coated silica particles

Controlled sedimentation of silica particles was previously reported by Jin et al.[61] Briefly, the bitumen-coated silica particles were mixed with toluene at ~2 wt% silica. The mixture was sonicated for 5 min and agitated using a magnetic stirrer (1100 rpm) for an additional 10 min. Then, a certain amount of additive, i.e., water, LGG and HGG, was introduced to the mixture, after which the mixture was stirred at 1100 rpm for 1 min and transferred to a 100 mL graduated cylinder. The changes of mudline location in the cylinder (mL) were recorded as a function of settling time (s). Figure 7 shows examples of sedimentation curves where the mudline location was plotted vs. time and initial settling rate (ISR) is determined from the initial slope of the curve. Turbidity of the supernatant after settling for 30 min was measured using Micro-100 Turbidimeter (Fisher Scientific, Canada) and expressed in NTU (nephelometric turbidity unit). Solid content in the supernatant was measured by centrifuging the supernatant at 5000 RCF for

10 minutes to separate toluene from the solids, then drying the solids in a fumehood for 3 h and finally weighing the resulting particles.[66]

3.5 FBRM measurement of water droplet in toluene and aggregate size

To determine the size of water droplets, the FBRM probe was immersed into a 250 mL beaker containing pure toluene. Water was gradually added to toluene during 1 h with constant stirring rate of 1100 rpm. To determine the size of solid particles, the FBRM probe was immersed in a 250 mL beaker containing a slurry of silica particles in toluene. Prior to FBRM measurements, the slurry was sonicated, stirred (1100 rpm) for 5 min. During the measurements, certain amount of additives, i.e., guar gum or water, were added to the slurry with constant stirring. The scanning laser of the FBRM probe was focused on a fine spot at the sapphire window interface and the reflected optical signal was processed. The corresponding chord length (s) was calculated as the product of the measured crossing time (Δt) and the beam velocity (Vb). Chord length counts are summed up in a finite number (number weighted: Number density) of chord length intervals, yielding the chords length distribution graphically.[67] Since the lens at the tip of the probe was 2.5 cm above the bottom of the beaker, continuous stirring was used during the measurements to avoid the settling of solid aggregates to the bottom.

3.6 Modification of FBRM measurement to follow the sedimentation of aggregates

Although under continuous stirring, tracking the settled aggregates of solid particles by FBRM measurements was still difficult due to the elevation of the probe. Therefore, the stirring speed was decreased to 20 rpm (minimum speed of the stirrer) in order to follow the aggregation process in a dynamic settling environment. Specifically, the slurry of bitumen-coated silica particles and toluene was stirred at 1100 rpm for 10 min and then the stirring speed was

immediately decreased to 20 rpm. The size of the aggregates was measured over time. When the FBRM probe could not detect the particles anymore, the settling was considered complete.

3.7 Water droplet size in pure toluene and cyclohexane

For the size measurement of water droplets in pure toluene and cyclohexane, the FBRM probe was immersed into a 250 mL beaker containing pure solvent and 0-3 vol % of water were added at constant stirring rate of 1100 rpm.

3.8 Water droplet effect on bitumen fine solids aggregation

A 1:25 vol. bitumen/solvent was prepared, sonicated for 5 min and agitated using a magnetic stirrer (1100 rpm) for an additional 10 min. Then, 0-3 vol.% of water were introduced to the mixture in a 250 mL beaker, maintaining the stirring rate. The scanning laser was focused to a fine spot at the sapphire window interface and this optical signal was then processed.

3.9 FBRM measurement of water and HGG induced aggregate formation

The effect of aromaticity is studied in aggregate formation. Mixtures of toluene/cyclohexane, that will be written as T/Ch, in 3:2 and 2:3 v/v were prepared. The FBRM probe was immersed into a 250 mL beaker containing the desired solvents mixtures, DI water droplets and HGG aqueous were added gradually (0.5-7.0 vol%) throughout 1h.

3.10 FBRM measurement of water and HGG induced aggregate formation before and after settling

Tracking the settling aggregates of solid particles by FBRM at high stirring speed, in addition to the elevation of the probe in relation to bottom of the beaker presents challenges. Therefore, the stirring speed was decreased from 1100 to 20 rpm (minimum speed of the stirrer)

in order to follow the aggregation process in a dynamic settling environment. Specifically, the slurry of bitumen/solvents with 0.75 vol% of DI water and HGG aqueous were stirred at 1100 rpm for 10 min and then the stirring speed was immediately decreased to 20 rpm. Two measurements were taken; the first one was taken immediately after the stirring speed was reduced, and the second measurement was done 5 minutes the first one.

3.11 Solid content determination by ashing and hot filtration

Ashing method was performed when the solid content in bitumen is above 0.2 wt%. In brief, about 3 g sample was poured in previously weighted crucibles, said crucibles have dried in the muffler oven at 775ºC before. The weight of the samples was recorded and the crucibles containing them are put inside the oven for 12 h at 80 ºC to ensure any residual solvent has been removed from the sample. The weight of the solvent free bitumen crucibles is recorded followed by introducing them back into the muffler oven and set to burn up to 775ºC for 3 h. The temperature is brought down by opening a small gap in the oven door. When the temperature of the oven reaches 200 ºC, the crucibles are placed in a glass desiccator to further cool down without losing or contaminating the sample. Finally, at 20ºC the last weight is recorded.

For solid content in bitumen product below 0.2 wt.%, hot filtration was performed. The sample is placed at 80 ºC in the oven for 24h to ensure any residual solvent is removed. In a clean 250 mL beaker containing 100 mL of toluene, 1 g of a solvent free sample is placed. The beaker is placed on a hot plate with an external temperature probe controlling the heat at 90°C. A second hot plate with external temperature control probe was used to heat another beaker of 300 mL of toluene at the same temperature. When the desired temperature is reached and the filter in place in the vacuum set-up, the filtration is started. The vacuum line is completely opened, and

the hot bitumen sample is transferred carefully to a filtration flask. Hot toluene is transferred to the sample beaker and is used to rinse all the bitumen into the filtration flask.

When the entire sample has been filtered, the remaining toluene is poured into the filtration receiving flask to rinse off the apparatus and the solids collected on the filter paper. The vacuum is left on for an additional 10min to dry out the filter paper, then the vacuum is shut off, the filter paper is transferred back to the aluminum sample holder, and it is placed in the oven at 115°C, this procedure was done previously to the filter paper without sample. After 10min, the filter paper and holder are removed from the oven and moved to the empty desiccator for 10min before attaining a final mass of filter paper, dish, and collected fines.

CHAPTER 4   RESULTS AND DISCUSSION

Two approaches are proposed to analyze the effectiveness of biomolecules, obtained from Guar beans, assisted settling of bituminous fine solids: A model and an industrial bitumen system. The model system is designed to analyze how hydrophilic additives such as DI water, LGG and HGG destabilize the surface of bitumen-coated silica particles in order to assist settling. On the other hand, the industrial bitumen system was design to apply the findings in the model system, in non-treated bitumen and at industrial settings, to study the feasibility of the proposed additive solution to further work at an industrial scale. Figure 7 shows the general experimental proceedings done in both approaches previously mentioned.
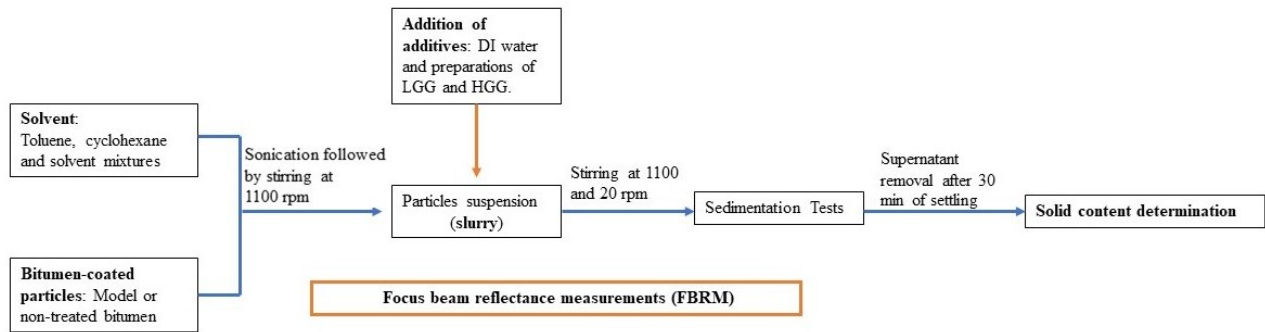
Figure 7. Schematic of the experimental procedure.

4.1 Destabilization of bitumen-coated fine solids in toluene through water assisted flocculation using biomolecules extracted from Guar beans

A model system in which pretreated bitumen-coated silica particles act as fine solids is used is this section. The analysis of DI water and Guar biomolecules -assisted settling is discussed while comparing the results of the settling rates, turbidity, and supernatant solid content.

4.1.1. Settling curves

Sedimentation tests of silica particles were conducted in toluene according to the previously reported method.[61,68] Figure 8 shows the settling curves, mudline position versus settling time, for both the bitumen-coated and bare silica particles. Most of the bare silica particles settled to the bottom of the graduated cylinder within one minute and the change of mudline reached an equilibrium state around 2 minutes, whereas bitumen-coated silica particles required almost 4 times longer settling time to finish the sedimentation. Previous work ascribed the result of bare silica particles to the size of the aggregates since hydrophilic silica particles tend to attract to each other in toluene due to their repulsion to the bitumen medium and its own strong interparticle adhesion. Conversely, the oleophilic bitumen-coated silica particles had good affinity to the bitumen media and the resulting steric repulsion between particles due to the swelling of bitumen layer in toluene could keep the particles apart.[69–71] Therefore, the suspension of treated silica particles was more stable than that of the bare silica particles.
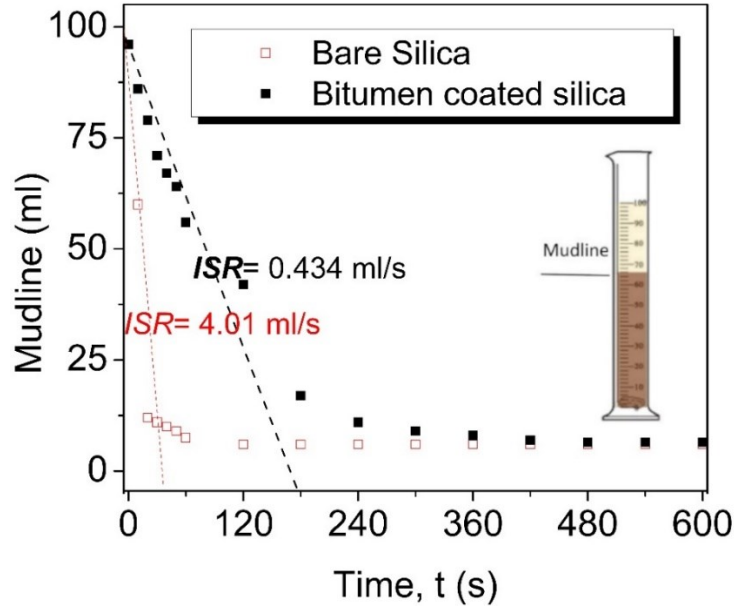
Figure 8 Settling curves of the bare silica particles (red void squares) and the bitumen-coated silica particles (black solid squares) in toluene. Insert: schematic of mudline in sedimentation tests in a graduated cylinder.

Settling curves were, also, obtained for LGG and HGG in toluene (Appendix B). Results from the settling rates are summarized in Table 1. In relation to bitumen-coated silica particles, high settling rates are found for LGG and HGG, this is due to the Guar gum's low solubility in organic solvents.[72] It can be observed that the addition of either LGG or HGG significantly improves the settling rate of the bitumen-coated silica particles. The size difference between the bitumen coated silica particles and LGG and HGG will also affect the outcome (Appendix C)

Table 1 . Initial settling rates of bare silica, bitumen-coated silica, LGG, HGG, bitumen-coated silica with 0.5 vol% LGG and 0.5 vol% HGG in toluene

System in toluene	ISR (mL/s)
Bare silica	4.010
Bitumen-coated silica	0.434
LGG	2.890
HGG	3.180
Bitumen-coated silica + 0.5 Vol % LGG	1.140
Bitumen-coated silica + 0.5 Vol % HGG	1.593

4.1.2 Sedimentation tests

4.1.2.1 Settling due to DI water droplets

Sedimentation tests with the addition of only water were conducted to investigate the effects of added water on destabilizing the bitumen-coated silica particles in toluene, and the results are shown in Figure 9A. An immediate increase in ISR and accompanying drop in supernatant turbidity were observed after a small amount of water (1 vol%) was introduced. The ISR continued to increase with the water dosage and then leveled off at about 5 vol% water. On the other hand, the supernatant turbidity reverted the decreasing trend when the water dosage was higher than 1.5 vol% and continuously increased with increasing water dosage.
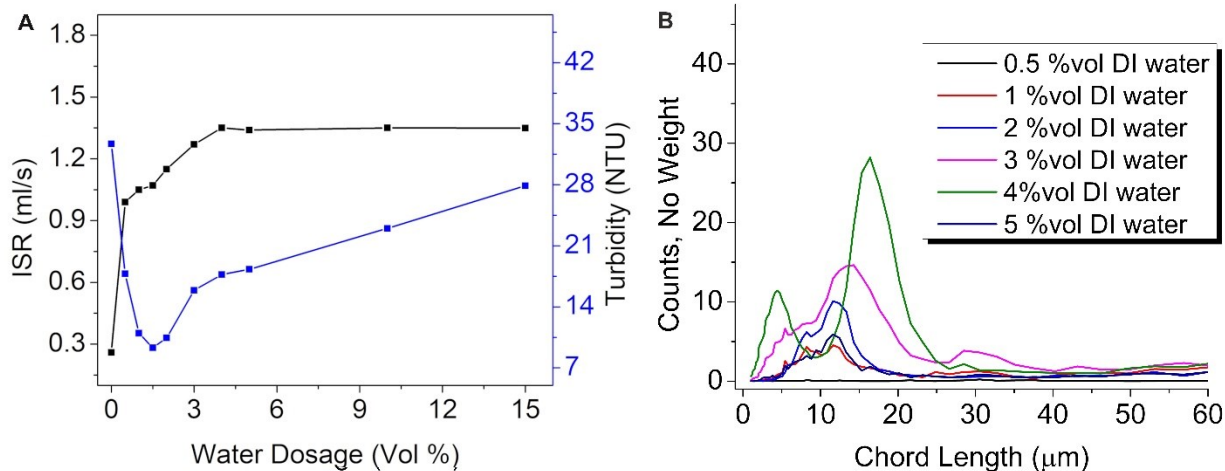
Figure 9 (A) Measured ISR and turbidity for particles in sedimentation tests with varied water content in toluene and (B) FBRM measurement of water droplet size in toluene as a function of water content.

Besides the degree of bitumen coatings, the size of water droplets could also affect the collision frequency of particles and the aggregation of particles with water droplets. FBRM measurements were applied to analyze the size distribution of water drops in toluene with varied water contents from 0.5 vol% to 5 vol%, and the corresponding results are shown in Figure 9B. At low water dosage of 0.5 vol%, the size of water drops was undetectable, and the counts was negligible. When water dosage was increased to 1 vol%, a broad size distribution from 4 to 30 µm was detected with a peak at ~ 12 µm. Such broad peak shifted to the higher chord length (i.e., as high as 18 µm) and the corresponding number counts increased simultaneously as the water dosage further increased from 1 vol% to 4 vol%, indicating an increase in both the size and the number of water droplets in the system. Further increase in water dosage (to 5 vol%) led to a sudden drop in both the size and the number of water droplets, likely due to increased coalescence of the water droplets. Based on the FBRM results, we speculate that the high turbidity values in the sedimentation tests specially as water content > 4 vol% could be ascribed to the rapid

coalescence of water droplets. Therefore, the added water did, in fact, destabilize the particles, however, not effectively since the formed large water droplets could instantly settle to the bottom.

4.1.2.2 Settling due to Guar gum

Figure 10A presents the results of sedimentation of bitumen-coated silica in toluene with the addition of only guar gums. For both LGG and HGG, the ISR value drastically increased upon the introduction of a small amount of toluene diluted guar gum (~ 0.5 vol%), and it then leveled off when the gum content was increased to about 3 vol%. The corresponding turbidity was found to fall sharply to 3.5 NTU and 6 NTU for HGG and LGG cases, respectively, at the gum dosage of 2 vol%. However, when the gum dosage further increased from 2 vol% to 15 vol%, the turbidity gradually climbed up to 8 NTU and 15 NTU for HGG and LGG cases, respectively. The increase in turbidity was possibly due to the increased concentration of residual gum in the suspension. It was noticed that the addition of HGG gave rise to higher ISR and lower turbidity values than the addition of LGG under all gum dosages, indicating the better performance of HGG in settling the particles. FBRM measurement showed that HGG could generate larger particle aggregates than the LGG obtaining a stable peak in between ~ 29-33 µm independent of the concentration (Figure 10B). Such results are attributed to the size of both LGG an HGG itself (Appendix D).
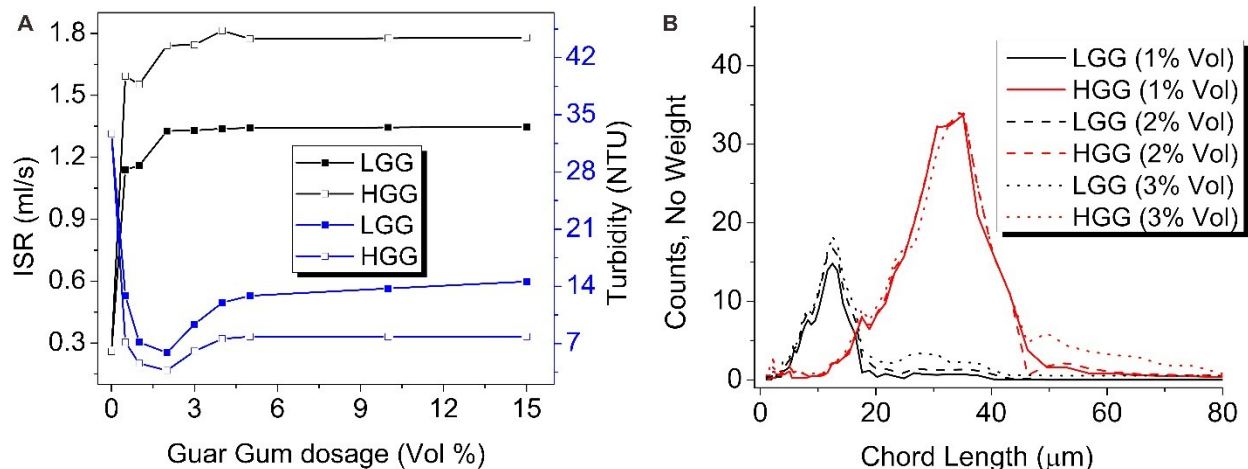
Figure 10 A) Measured ISR and turbidity for the 1B5S in sedimentation tests with varied content of LGG (solid square) and HGG (void square) in toluene and B) FBRM results of the solid particles in toluene with the addition of LGG (black) and HGG (red) with varied dosages.

The effect of the addition of guar gum, both LGG and HGG at 0.5 vol% can be observed in Figure 11. The clarity of the supernatant is responsive to the type of additive added. When comparing the results from Figure 11B and 11A, the supernatant shows less turbidity to the naked eye as a result of using LGG. However, better results can be observed when HGG is added to the bitumen-coated silica in toluene solution. Clarity of the supernatant remarkably increased, not only from the untreated sample, but the LGG treated sample as well.
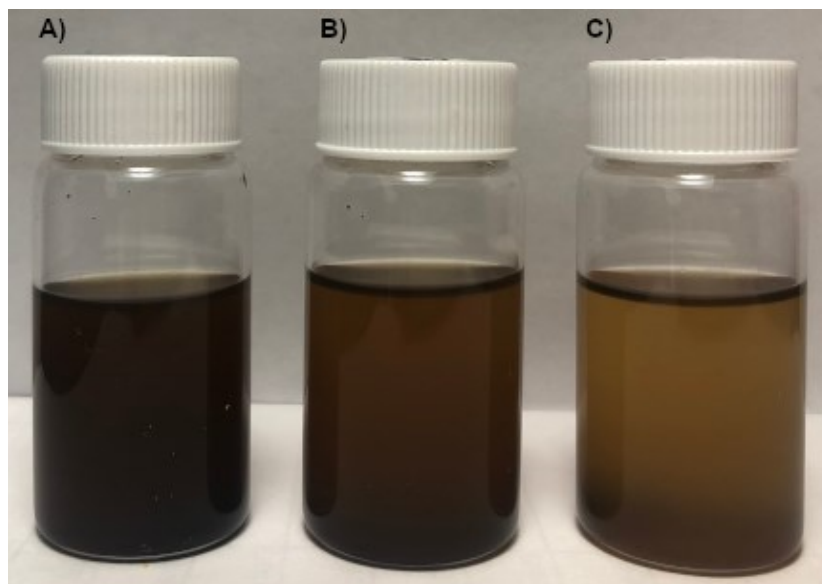
Figure 11 Photographs of settling samples when the bitumen-coated silica in toluene solution is A) untreated and treated with 0.5 vol% of B) LGG and C) HGG are added, after 10 minutes of settling.

Sedimentation tests with the addition of both guar gum and water were also conducted. Figure 12 shows the results with the addition of the guar gum aqueous solutions. As can be seen, for the LGG, the use of its aqueous solution exhibited the similar settling performance to the use of itself without water (Figure 10A). In other words, the combined addition of LGG and water could reduce the amount of LGG necessary to achieve a desirable result. It can also be seen that the use of LGG aqueous solution exerted an apparent reduction in the turbidity of the supernatant compared with the water only case. This suggests that the combined addition of both LGG and water could strengthen the interactions between the added water and the bitumen-coated silica particles suspended in toluene. The possible reason is that the LGG, an amphiphilic chemical, could migrate to the water/bitumen interface, and the hydrophobic segments facing the bitumen phase could induce attractive force between the water droplet and solid particles. On the contrary, the addition of HGG aqueous solution caused a slight decline in ISR in comparison

with the addition of HGG alone. The effectiveness of the HGG aqueous solution on decreasing the supernatant turbidity was also inferior to that of the LGG, and the minimum turbidity was found to be ~ 8 NTU for the HGG aqueous solution and ~ 3.5 NTU for HGG only. These results are reasonable because the HGG can be easily hydrated by water molecules through strong hydrogen bonding due to numerous hydroxyl groups across the chain of HGG deteriorating the affinity with bitumen coated silica particles. As a result, the migration and diffusion of HGG to the water/bitumen interface would be limited and the flocculation of solid particles by HGG would be weakened in addition to having a lower concentration of the gum, since it is diluted in DI-water.
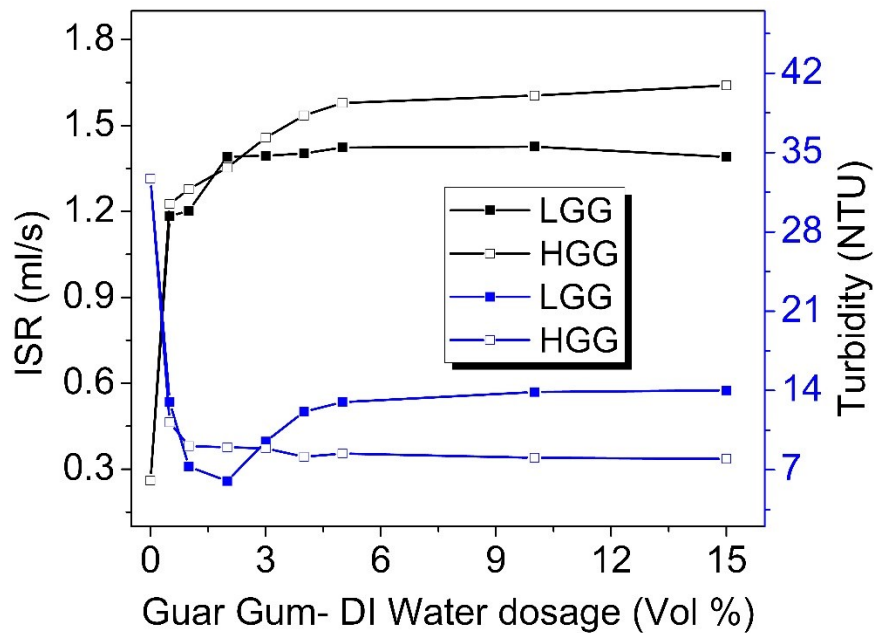
Figure 12 Measured ISR and turbidity for the 1B5S in sedimentation tests with varied content of LGG aqueous solution (solid square) and HGG aqueous solution (void square) in toluene.

Considering the ISR and turbidity data and gum dosages, it can be concluded that the ability of these additives to destabilize the bitumen-coated silica particles followed the order: water < LGG < LGG aqueous solution < HGG aqueous solution ≈ HGG. The trend can be

reasonably explained based on the distinct chemical structures of the two gums and their different destabilization mechanisms. The amphiphilic LGG serves as a modifier to the water/bitumen interface to induce the strong adhesion between the water drops and the hydrophobic bitumen-coated silica particles. The gum dosage was much higher when the LGG was used alone than when it was used as an aqueous solution, and the inferior results even at the higher dosage was possibly due to the insoluble nature of the LGG in toluene. Therefore, in the case of the added LGG aqueous solution, the water drops provided suitable water/bitumen interfaces for the LGG, where the gum was enriched which promoted the interactions between the LGG and solid particles. In contrast, the introduction of water to the HGG system would heavily block the HGG in water drops not significantly improving the flocculation efficiency.
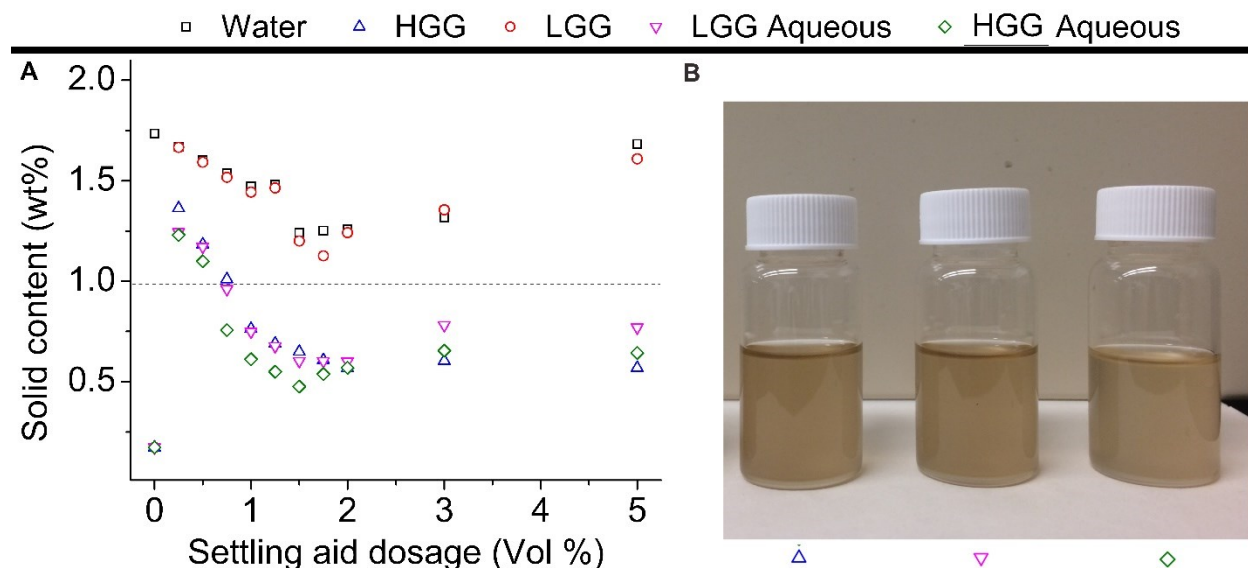
Figure 13 A) Solid content in supernatant after 30 min settling achieved with the addition of only water (black), LGG (red), HGG, (royal) LGG aqueous solution (magenta) and HGG aqueous solution (olive), and B) photographs of supernatant samples with addition of 1.5 vol% of HGG, LGG aqueous solution and HGG aqueous solution, respectively.

To have a better view of the performances of these additives, the residual solid content retained in the supernatant after 30 min settling was determined. Figure 13A presents the collected data from the five types of batch tests with the dosages of additives from 0 vol% to 5 vol%. Overall, the cases of only water and only LGG showed much higher solid contents than other three cases under all dosage conditions. The performance of LGG was visibly enhanced once it was added to the solid-toluene slurry in the form of aqueous solution, and the minimum solid contents were found to be ~ 1.1 wt% and ~ 0.6 wt% for the LGG and LGG aqueous solution, respectively, which was consistent with the turbidity and ISR results.

Regarding HGG, the introduction of water did not improve the performance. However, at additives dosages of 0.2-1.8 vol%, the solid content was slightly lower in the case of HGG aqueous solution than in the case of HGG, this is not considered significant due to a standard deviation of ± 0.01 wt%. Interestingly, the performances of LGG aqueous solution, HGG and HGG aqueous solution on reducing the solid content were found to be identical at 2 vol% dosage condition and their supernatant sample exhibited the similar clarity at 1.5 vol%, as observed in Figure 13B.

4.1.3 FBRM measurements

4.1.3.1 Aggregates' size during constant stirring

FBRM was used to have a clear assessment of the dimension of aggregates of bitumen-coated silica particles formed during the dynamic stirring process. Figure 14A and Table 2, present the size distribution of aggregates recorded upon the addition of only water, LGG, HGG, LGG aqueous solution and HGG aqueous solution. The dosage of all the additives was fixed to 1.5 vol%. The case of LGG showed a broad size distribution (5-45 μm) and most of the aggregates' size was concentrated in the 21-30 μm range. In comparison, the addition of LGG

aqueous solution resulted in a more defined unimodal distribution with higher counts, indicating that more solid particles experienced aggregation and that water is imperative, in this case, to form aggregates. The resultant peak was found higher chord length (~ 11-30 µm) and most of the peak area overlapped with the peak of water drops, suggesting that most of the particle aggregates were possibly captured by water drops, with the enhancement caused by the appearance of LGG on the water/bitumen interface. For HGG, the size distribution of adding HGG only exhibited unimodal distribution withing the largest ranges (11-80 µm), accounting for the formation of large solid flocs by polysaccharide. The peak location slightly shifted to the right when using the HGG aqueous (31-80 µm) solution as the additive.
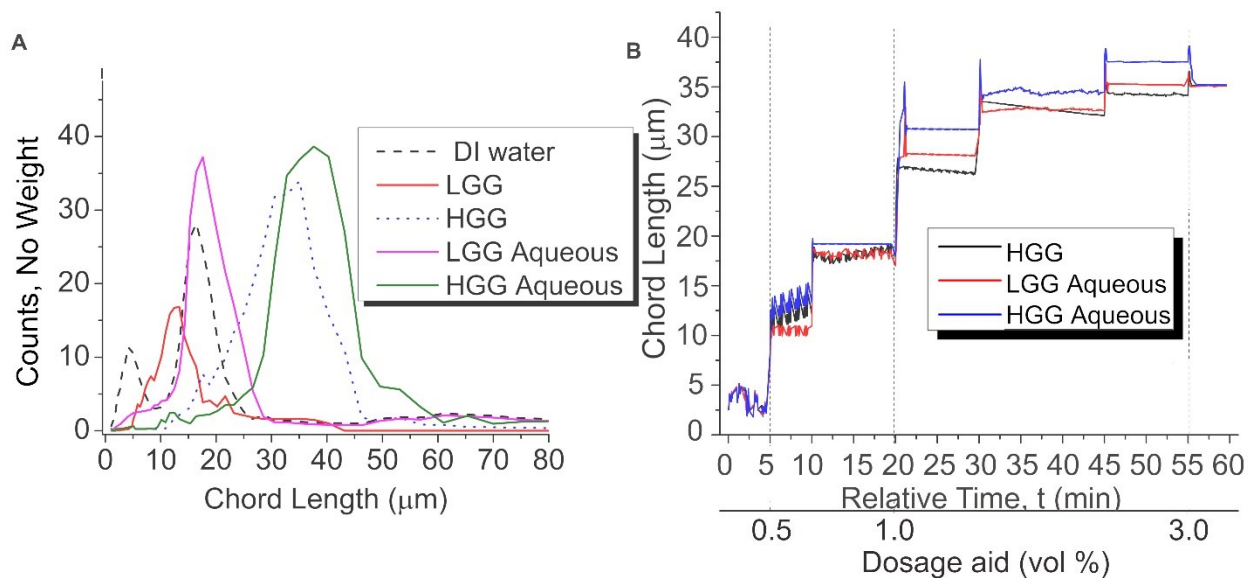
Figure 14 A) Chord length versus counts measured by FBRM using a fixed dosage of additive at 1.5 vol%. B) Mean Chord length versus time, according to the additives' dosage with the sequential addition of HGG, LGG aqueous solution and HGG aqueous solution The mixing speed was kept at 1100 rpm.

Table 2 Total counts of aggregates after introducing 1.5 vol% of DI water, LGG, HGG, LGG aqueous and HGG aqueous, at a constant stirring speed of 1100 rpm.

Total counts (No Weight)

Chord length (μm)	DI water	LGG	HGG	LGG Aqueous	HGG Aqueous
1 to 10	181	46	12	51	11
11 to 30	179	55	229	256	79
31 to 80	22	12	143	19	222

Figure 14B shows the changes in the size of aggregates upon the sequential addition (0.5, 0.75, 1.0, 1.5, 2.0 and 3.0 vol%) of HGG, LGG aqueous solution and HGG aqueous solution, respectively. It was clearly noticed that each subsequent addition of gum or gum aqueous solution led to a significant increase in aggregate size. For example, from 5 min to 20 min, as the dosage of HGG increased from 0.5 vol% to 1 vol%, the mean chord length was apparently changed from 12 to 27 μm, indicating a further aggregation of suspended solid with the flocs formed previously. For the cases of LGG aqueous solution and HGG aqueous solution, the subsequent addition at 20 min resulted in a more apparent change in mean chord length, which can be attributed to the generation of large water-solid agglomerates. From 20 min to 55 min, with the dosage further increasing to 3 vol%, the mean chord length also showed obvious increase after each addition. When the dosage was above 3 vol%, the cases of HGG and LGG aqueous solution did not present further growth in chord length, while the case of HGG aqueous solution experienced a slight decline in the mean chord length possibly due to the collapse of large aggregates under the strong external mechanical stirring (1100 rpm).

4.1.3.2 Aggregates' size during settling process

FBRM measurements with low stirring speed (20 rpm) were applied to monitor the in-situ size of aggregates during the sedimentation process. Figure 15A shows the changes of chord length as a function of time with the addition of water, LGG, HGG, LGG aqueous solution and HGG aqueous solution. Without the enough agitation, the formed large aggregates would quickly settle. Consequently, the size of aggregates suspended in toluene would continuously decrease and ultimately became negligible once the settling was completed.
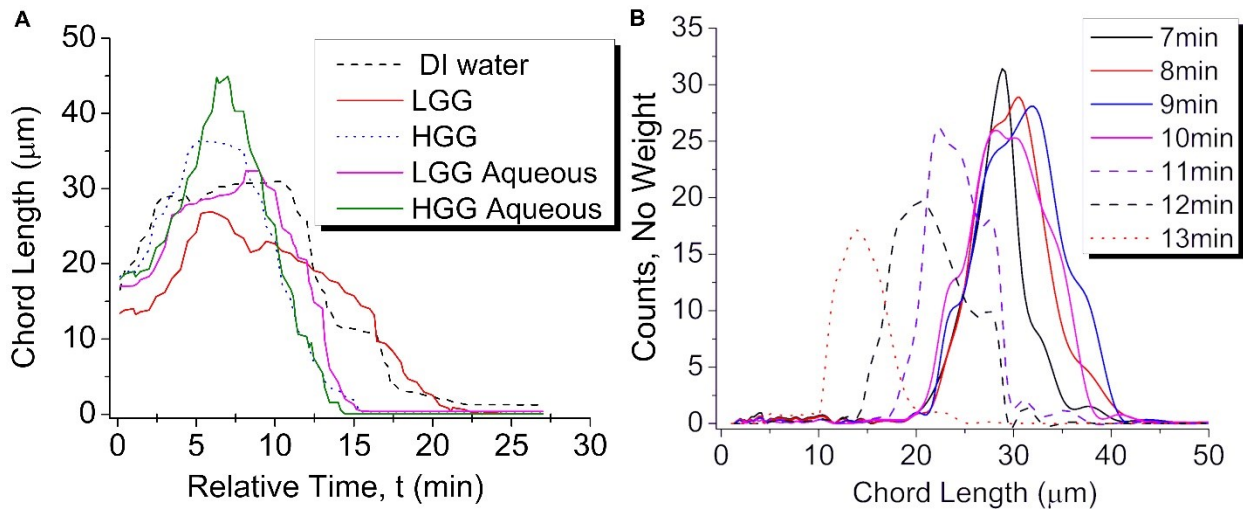
Figure 15 A) Chord length versus time using a fixed dosage of all additives of 1.5 vol% and B) Size distribution during settling using LGG aqueous at the same fixed dosage, measured by FBRM in the slurry. The stirring speed was kept at 20 rpm.

According to the results in Figure 15A, two kinds of decline behaviors were observed: a steep decline and a mild decline. Apparently, the addition of HGG, LGG aqueous solution or HGG aqueous solution showed the steep decline in aggregate size, and the settling was completed around 15 min, which were in good agreement with the relatively high ISR values achieved in these three cases. It is interesting to note that although the size of aggregates in the case of LGG aqueous solution did not go beyond 35 μm, it had a slightly steeper slope than

HGG, suggesting that most of the aggregates formed in this case had the same size and there was little breakage during settling due to the small amount of water confirmed by the size distribution taken during settling shown in Figure 15B, on the other hand the size distribution for HGG systems show a broader size distribution (Figure 16). For the addition of water only or LGG only which showed low ISR and high residual solid content in sedimentation tests, a mild decline in the size of aggregates was observed. Under such low stirring rate (20 rpm), the pure water droplets would undergo coalescence and became unstable. Consequently, the aggregates formation was only attributed to collision between particles in the case of only water.
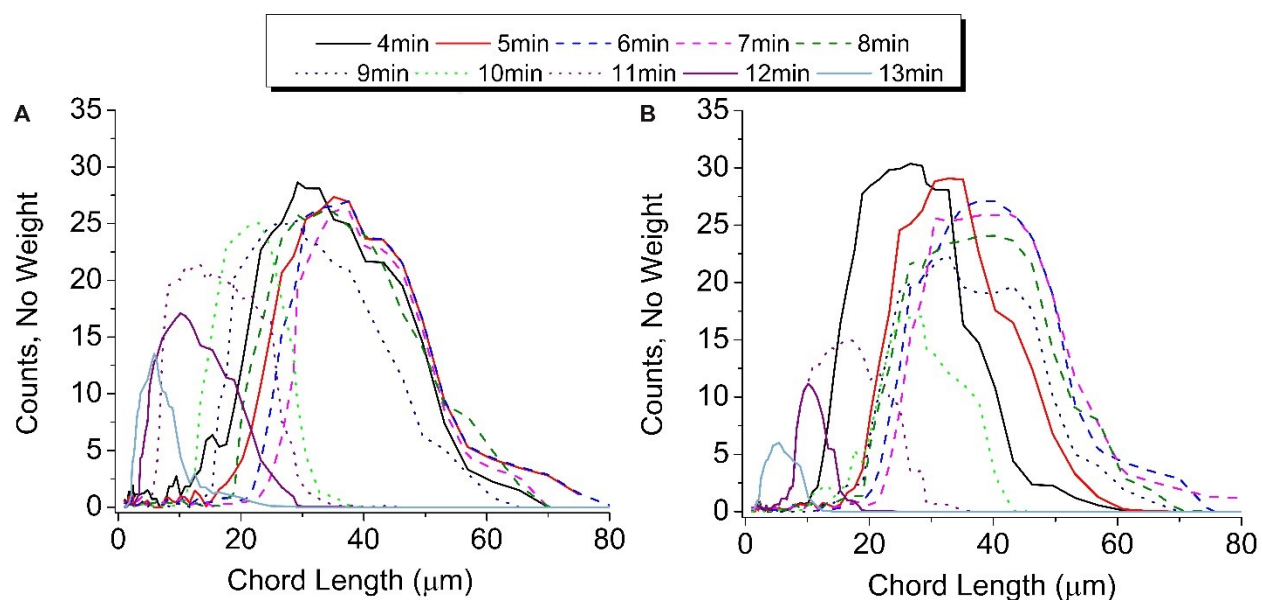
Figure 16 FBRM Size distribution during settling time for A) HGG and B) HGG aqueous at a dosage of 1.5 vol%. The stirring speed was kept at 20 rpm.

4.2 Effect of aromaticity in the destabilization of fine solid present in untreated bitumen through water-assisted flocculation using high molecular weight Guar gum

The effect of aromaticity in the destabilization of fine solids to further flocculate with DI water and Guar biomolecule is studied by using two good solvents (toluene and cyclohexane) and the mixture. The results gathered in the previous section led to the study of systems with DI

water and HGG aqueous in diluted indigenous Athabasca bitumen. The original water content of the sample was 0.013 wt%, measured according to Fischer titration.

4.2.1 Size distribution of DI water droplets in pure and bituminous media

4.2.1.1 Size distribution of DI water droplets in pure toluene and cyclohexane

Desired amount of water was added to toluene and cyclohexane stepwise from 0.5, 1, 2 to 3 vol% at constant stirring speed of 1100 rpm while the FBRM probe was immersed in the solution to measure droplet size. As shown in Figure 17, droplet stability varies significantly between both solvents.
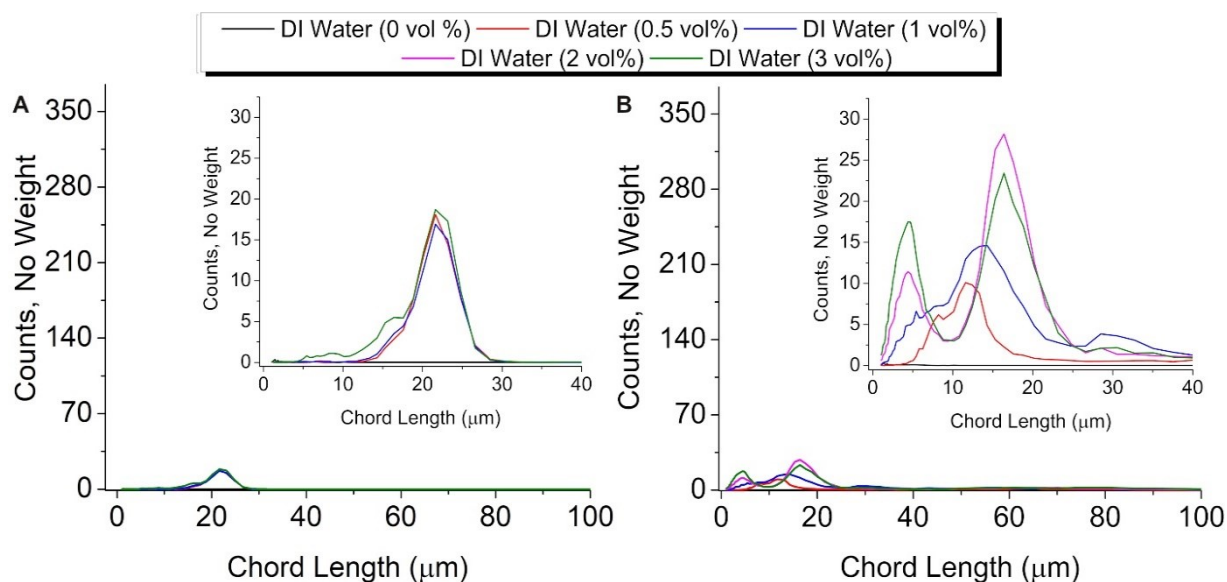
Figure 17 FBRM measurements of DI water droplet formation in A) Cyclohexane and B) Toluene.

Overall, the size of water droplets in cyclohexane is predominantly in the range of 10-30 µm with a unimodal distribution, and water cannot be dispersed well in cyclohexane (a phase separation might occur even at such high mixing speed). In toluene, a bimodal distribution was observed with increasing DI water concentration. The peak in the 10-30 µm range is similar to

cyclohexane, indicating unstable emulsion droplets, while peaks in the range of 1-10 μm likely indicate the stable water-in-oil emulsion. This is theorized to be due to the difference in the solubility parameter; for cyclohexane is 16.8 MPa and 18.3 for toluene.

4.2.1.2 Water droplet size in bituminous toluene and cyclohexane

Each solvent is separately added to bitumen in a 1:25 bitumen to solvent volume ratio followed by the addition of water droplets. Figure 18 shows the FBRM measurement results in this system. Compared with Figure 17, a shift to lower chord length is observed. This may be caused by the presence of fine solids in the bitumen, and/or by the emulsion stabilization capability of the bitumen components. Without the addition of water (black line), the size distribution of fine solids is comparable in both solvents with a mean value of ~5 μm. By adding water, the results start to differ accordingly. In the cyclohexane/water/bitumen system (Figure 18A), aggregate size distribution shifted to the left gradually by increasing the water concentration. All fine particles are in a water-in-oil emulsion form at above 2 vol% water concentration, resulting in a disappearance of unimodal distribution of fine particles. In contrast, addition of water has two contributions to the toluene/bitumen (Figure 18B): (1) A similar chord length distribution to fine solids from 1 – 20 μm with much higher counts. (2) Similar to water droplets in pure toluene, between 10-40 μm but with a higher intensity in the counts. Overall results suggest that the water forms a relative stable emulsion in bitumen/toluene/fine solids as the size of water droplets are smaller than that in cyclohexane.
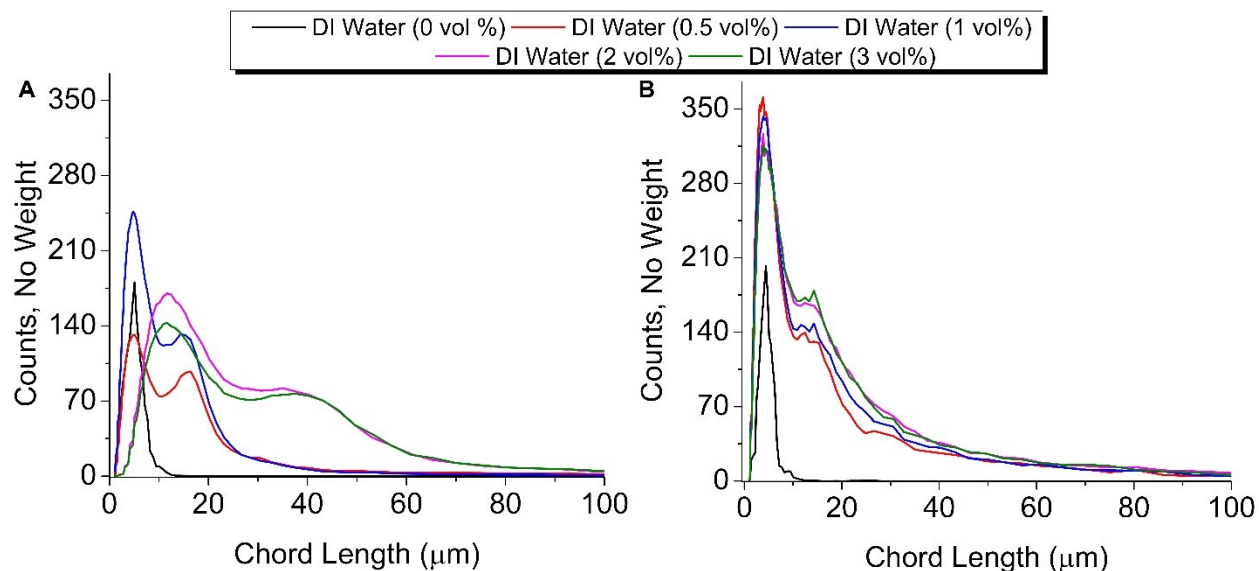
Figure 18 FBRM measurements of DI water droplet size in bituminous A) Cyclohexane and B) Toluene.

4.2.2 HGG aqueous settling curve

Due to good performance in the controlled settling tests, with bitumen-coated silica, HGG aqueous is used to further test its effectiveness when modifying aromaticity. The sedimentation tests were conducted in DI water, toluene and cyclohexane (Figure 19).[61,68] In toluene and cyclohexane, most of the HGG settled to the bottom of the graduated cylinder within 1 minute of the test and the change of mudline reached the equilibrium state after 2 minutes, whereas the stable suspension of HGG in water does not settle during the measured time due to high solubility. However, the HGG-water system does show a negative slope.

Studies related to HGG have reported its solubility in water and other solvents with high content of hydroxyl groups.[73,74] Therefore, low to no solubility is expected from HGG in toluene and cyclohexane,[75] however, even though the settling test was performed several times (6 repetitions), the settling rate obtained of HGG in toluene and cyclohexane show a negligible difference. This indicates that aromaticity will not affect the stability of HGG in the solvent.

Therefore, is expected that the settling rates of HGG in toluene/cyclohexane mixtures will not deviate from the ones obtained in the pure solvents (Appendix E).
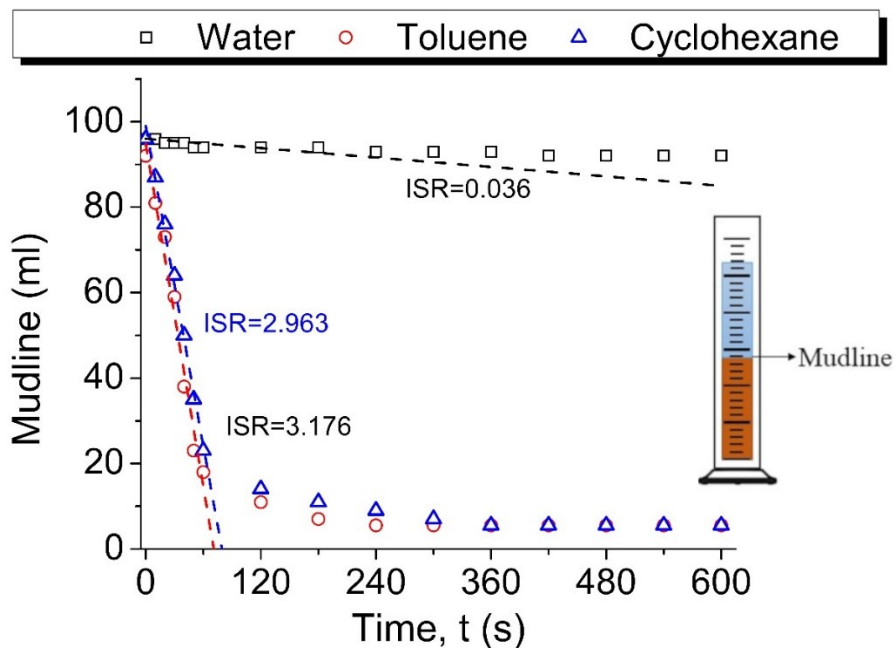
Figure 19 Settling curves of high molecular weight Guar gum (HGG)in aqueous solution in water (black void squares), toluene (red void circles) and cyclohexane (blue void triangles). Insert: schematic of mudline in sedimentation tests in a graduated cylinder

4.2.3 Aromaticity effect on size distribution of pure and bituminous systems

4.2.3.1 Aromaticity effect on water droplets and HGG aggregates' size

A mixture of solvents is proposed to analyze the implication of aromaticity when using a hydrophilic aid to accelerate the settling process. In Figure 20, formation and mean size value of water droplets and HGG aggregates in pure and mixed solvent systems can be observed. In Figure 20A, the effect of water addition is shown. In the cyclohexane system, the data supports our previous results without a significant variation in the mean chord length of the droplet, and size changes in form of peaks are only seen when increments of water are introduced. On the

other hand, increasing the water content in toluene increases the mean size of the water droplets in discrete steps for dosages between 0.5-1.5 vol%. In mixed systems, mean aggregate sizes slightly increase with the increment in water dosage from 0.5-1.0 vol%. Considering the structure and insolubility of HGG in organic solvents, larger chord lengths are expected and observed (Figure 20B).[76] The chord length of the HGG aggregates in pure toluene and mixtures, in terms of HGG dosage, follows the same tendency as of water droplets. However, a clear shift in the overall order of the mean chord length is observed. Mean aggregate size in cyclohexane have the smaller chord length and the behavior throughout the addition of HGG varies independently of the dosage added.
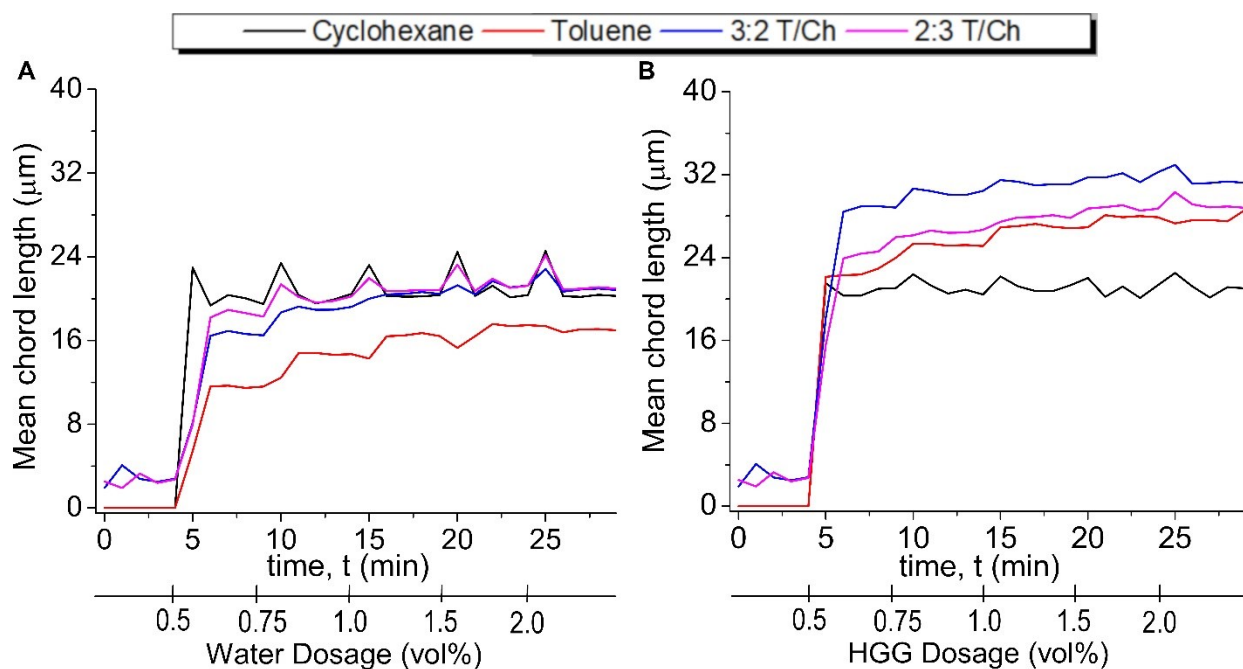
Figure 20 Effect of solvent and solvent mixture on aggregate formation varying the amount of A) DI water and B) HGG dosages.

Overall, aggregates' mean size values stay constant independently of the amount of HGG aqueous added to the system, apart from the peaks from the initial introduction of the aid. Interestingly, solvent mixtures seem to help stabilize larger HGG aggregate sizes.

Table 3 shows the mean chord length and total No Weight counts of DI water droplets and HGG aggregates formed when 0.75 vol% of each additive is added to toluene, cyclohexane and solvent mixtures. In agreement with the results showed in Figure 20, lower counts of HGG aggregates are obtained due to longer chord length, suggesting less breakage during collisions induced by constant stirring.

When additives are introduced to pure toluene, a clear difference of almost 39% between water droplet counts and HGG aggregate counts is observed. In contrast, the cyclohexane system not only shows that the HGG aggregate sizes are larger than water droplets but, the count of HGG aggregates is also higher than water droplets. This suggests that a) DI water in cyclohexane forms very few droplets above the mean chord length values and/or b) HGG aggregate chord lengths are less uniform.

Table 3 Mean Chord lengths and Total counts of DI water droplets and HGG aggregates when 0.75 vol% of each additive is added to toluene, cyclohexane and solvent mixtures, without bitumen.

Solvent	Mean chord length		Total counts (No Weight)	
	DI water	HGG	DI water	HGG
Toluene	12.45	25.32	159	97
Cyclohexane	21.81	22.38	94	98
3:2 T/Ch	18.70	30.66	120	93
2:3 T/Ch	21.36	26.16	113	96

In addition, Table 3 shows the total counts and size of droplets and aggregates in 3:2 T/Ch and 2:3 T/Ch. Both results show that there is a smaller number of HGG aggregates than water droplets, agreeing with the mean chord lengths obtained. The sizes of the HGG aggregates were 1.64 and 1.22 times larger than the water droplets in 3:2 T/Ch and 2:3 T/Ch, respectively. The mixed system with higher toluene concentration has the least number of HGG aggregates counts overall.

Independently of the solvent or solvent mixture, the mean chord length of HGG aggregates is higher than the size of water droplets. The water droplet mean chord length follows the order: toluene < 3:2 T/Ch < 2:3 T/Ch ≈ cyclohexane. On the other hand, HGG aggregate mean chord length follows the order: cyclohexane < toluene ≈ 2:3 T/Ch < 3:2 T/Ch.

4.2.3.2 Aromaticity effect on the aggregate size in bituminous slurry

Solvent-diluted bitumen slurries (bitumen in toluene, cyclohexane and solvent mixtures) are prepared, DI water and HGG are introduced to each system, and the stirring speed is reduced from 1100 to 20 rpm. After the previous tests, 0.75 vol% of additive is chosen to be added in the following experiments. Aggregate and droplet size distribution at 0.75 vol% are comparable for all solvent systems with a low consumption of the additives.

To analyze aggregate formation after stirring and during settling, two measurements are taken: one measurement is done immediately after the stirring speed is reduced and the second measurement is taken at 5 minutes after the first measurement. As shown in Figures 21 and 22, total counts reduced notably independent of the additive or the solvent, decreasing in 51% and 69% in cyclohexane and toluene, respectively (from Figure 18 and Appendix F). In addition, Tables 4 and 5 provide where the total counts (No Weight) are distributed into three distinct ranges 1-10,

11-20 and 21-60 µm. Due to the large reduction in total counts, significant counts will be considered above 200, which is approximately the 10% of the untreated bitumen sample.

In Figure 21, aggregate formation and settling with water as the chosen process aid is observed. Figure 21A shows the size distribution of aggregates right after the stirring speed was reduced. Significant counts can be found between the 11-60 µm ranges, in pure cyclohexane, having comparable counts in both the 11-20 and 21-60 µm ranges. The pure toluene system shows high aggregate counts in the smaller chord length range, especially in the 1-10 µm size range. In mixed solvent systems, a higher content of toluene results in the defined peak in the smaller chord lengths (~5-12 µm), although the sum of the aggregates in the other range (21-60µm) can be considered significant. When the content of cyclohexane surpasses toluene (2:3 T/Ch), significant counts can be found between 1-20 µm, but this system had a considerably higher number of aggregates in the larger size range (21-60 µm) than toluene and 3:2 T/Ch. Although a significant amount of aggregates below 20 µm was observed in both T/Ch solvents, the result of 3:2 T/Ch approximately resembles that of toluene, while that of 2:3 T/Ch resembles that of cyclohexane. Despite the considerable decrease in the amount of aggregates, cyclohexane containing systems appear to have, on average, slightly higher counts of aggregates.
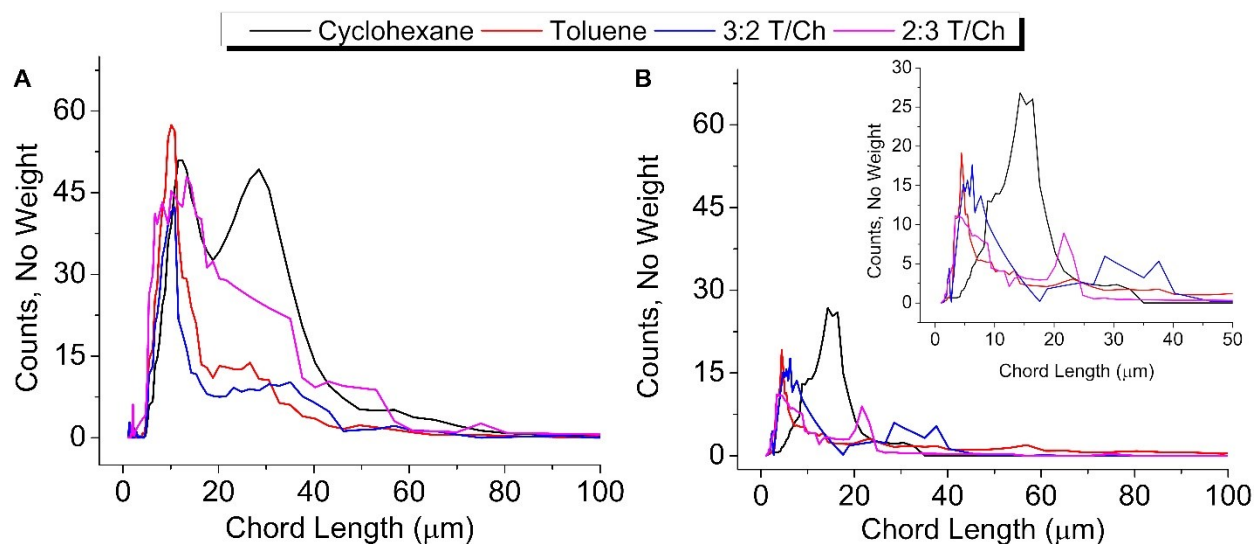
Figure 21 FBRM results of effect of solvent and solvent mixture on aggregate formation with 0.75 vol% of DI water immediately after stirring, A) before settling and B) after 5 minutes of settling.

After 5 minutes of settling significant reduction of counts are found in all solvent systems as shown in Figure 21B and Table 4. However, results in mixed solvents show fewer counts of aggregates in a broader range of sizes (>10 μm), compared to the results for pure solvent systems. The majority of the aggregates in the cyclohexane system are in the 11-20 μm range, although a comparable number of aggregates can be found in the upper limit of the lower range (1-10 μm). Most aggregates in toluene continue to be present between 1-10 μm in addition to having significantly smaller counts of aggregates up to 60 μm.

Table 4 Total counts of aggregates after introducing 0.75 vol% of DI water when stirring speed is reduced to promote settling and after 5 minutes of settling, in toluene, cyclohexane and solvent mixtures.

	Total counts (No Weight)							
	Before settling				5 min after settling			
	Chord length (μm)			Total	Chord length (μm)			Total
Solvent	1-10	11-20	21-60		1-10	11-20	21-60	
Toluene	350	248	107	705	111	60	78	249
Cyclohexane	200	420	409	1029	92	180	19	291
3:2 T/Ch	272	156	102	530	178	27	29	234
2:3 T/Ch	250	235	163	648	191	35	22	248

The previously described procedure is repeated with HGG obtaining the results shown in Figure 22 and Table 5. Overall, most significant counts were found the small size range. In Figure 22A, aggregates in pure toluene have higher counts in a short range of small chord lengths (~3-20μm) contrary to aggregates in pure cyclohexane which have a wider range of sizes (~8-35μm), however, lower counts overall, this being the main difference with water aided aggregates. In mixed systems, random peaks above 50μm can be found. In the 3:2 T/Ch system, an array of chord lengths varying from ~5-90μm is observed, yet, significant counts from this system are found principally from ~5-27μm. In 2:3 T/Ch, a standalone peak in ~5μm followed by a count-decreasing peak ranging between ~8-36μm are identified, however, significant counts are also observed in ~53μm.
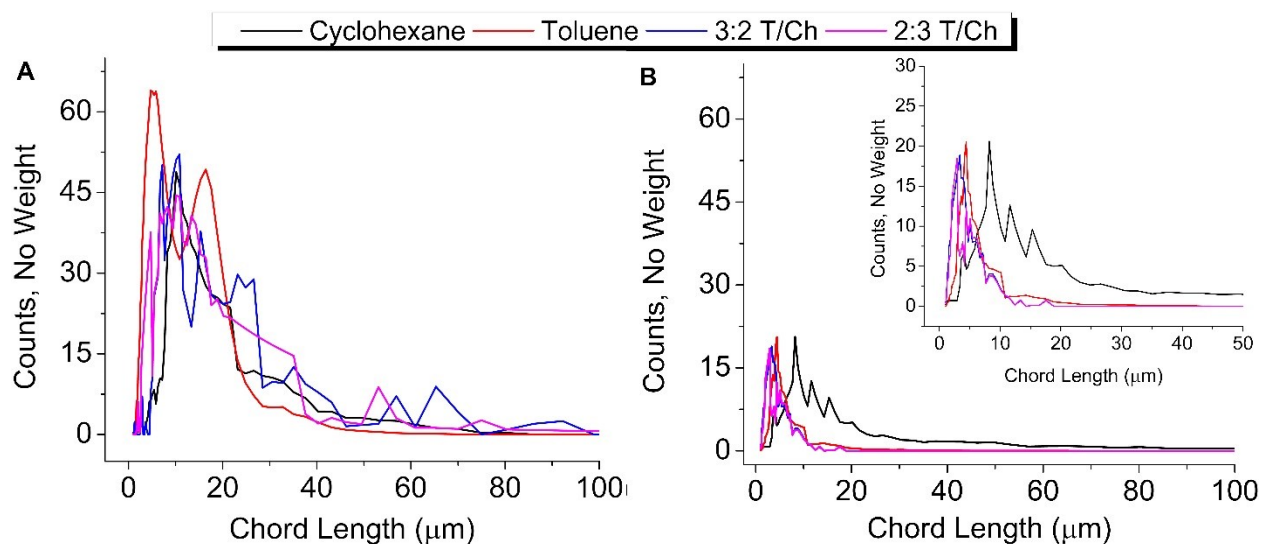
Figure 22 FBRM results of effect of solvent and solvent mixture on aggregate formation with 0.75 % Vol of HGG aqueous immediately after stirring, A) before settling and B) after 5 minutes of settling.

Once again counts in all systems have decreased considerably after 5 minutes of settling. When comparing Figure 21B and 22B, HGG accelerates the settling because of high molecular weight inherit to HGG,[75] hence lower counts are observed in all systems with a more uniform size. The pure cyclohexane system, similarly, to the results with water as a settling aid, has larger aggregates (~5-21µm) that due to its size can be expected to settle in the next few minutes. The number of aggregates in pure toluene are comparable with the ones found in pure cyclohexane, however, the chord length (~3-9µm) is still very small. In mixed systems, both showed slightly fewer counts than pure solvent results, with an average chord length has a uniform tendency (~2-8µm).

Table 5 Total counts of aggregates after introducing 0.75 vol% of HGG aqueous when stirring speed is reduced to promote settling and after 5 minutes of settling, in toluene, cyclohexane and solvent mixtures.

	Total counts (No Weight)							
	Before settling				5 min after settling			
	Chord length (µm)			Total	Chord length (µm)			Total
Solvent	1-10	11-20	21-60		1-10	11-20	21-60	
Toluene	244	310	122	676	160	8	1	169
Cyclohexane	674	243	49	966	159	75	39	273
3:2 T/Ch	265	142	77	484	146	2	0	148
2:3 T/Ch	239	160	113	512	152	3	0	155

The size and quantity of fine solids (FS) and aggregates (Agg) can be appreciated in Figure 23, where microscopic imaging of the results, both after stirring speed is reduced and 5 minutes of settling when HGG is used are shown. Figure 23 A-D shows the solids in the supernatant taken immediately after the stirring rate was reduced to 20 rpm, while Figure 23 E-H presents the images of the supernatant taken after 5 minutes of settling. Overall, Figure 23 validates the results found in the FBRM tests for HGG-treated solvent-diluted bitumen. The presence of large aggregates (> 30µm) when solvent mixtures are used after the stirring speed is slowed down is observed in Figure 23 C and D. This confirms the peaks found between the 30-40µm chord lengths shown in Figure 22A. After 5 minutes of settling, the supernatants contain less aggregates as shown in the microscopic images, which is consistent with the low counts measured in the FBRM tests. In addition, the system with higher counts appears to be cyclohexane.
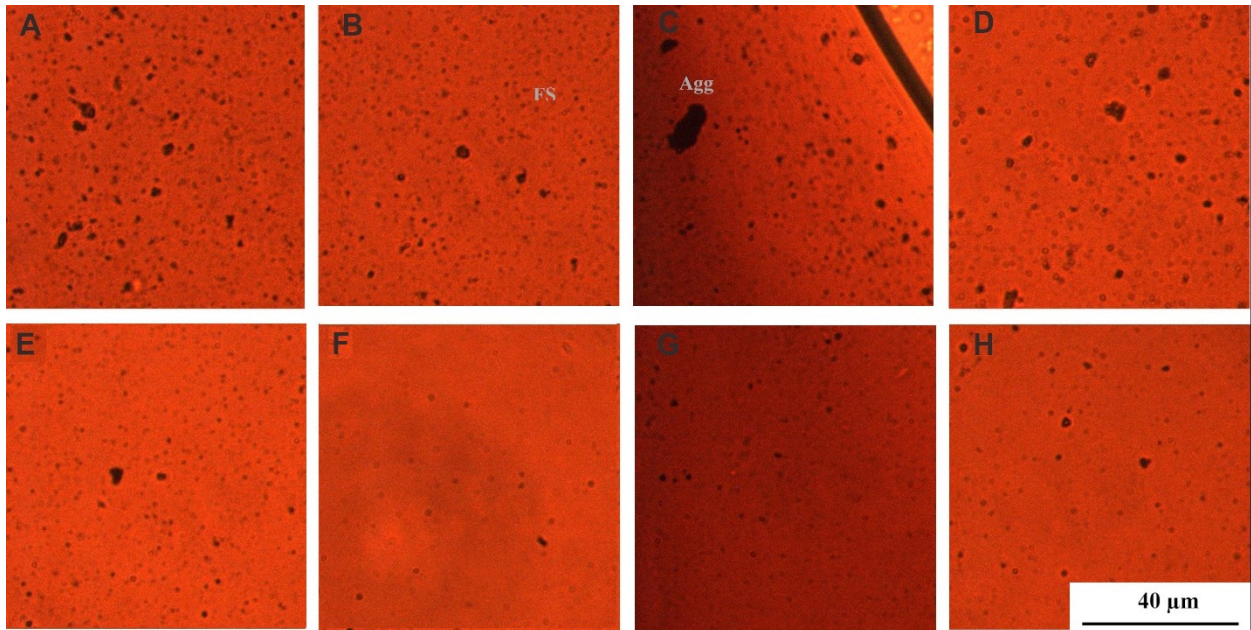
Figure 23 Micrographs of supernatant after treating the slurry with 0.75 % Vol of HGG aqueous A-D) immediately after stirring and E-H) after 5 minutes of settling; (from left to right) in cyclohexane, toluene, 3:2 T/Ch and 2:3 T/Ch, respectively.

4.2.4 Solid content determination in supernatant after settling

4.2.4.1 Solid content: DI water and HGG effect

In accordance to resident time in industrial settling tanks, supernatant samples are taken after 30 minutes of settling. Ashing protocol and hot filtration are performed to obtain the final solid content.

As shown in Figure 24, in the control experiment without additives, the solid content in bitumen kept constant independently of the solvent measured. When the water or HGG was added, the solids content in bitumen decreased. The addition of water has shown the benefit on the reduction of solid contents in bitumen, while a slight better performance was observed in

mixed solvents than pure solvents. On the other hand, the addition of HGG has shown a remarkable reduction in solid content in all solvents, particularly in mixed solvents, which was verified by both ashing and hot filtration methods. Among the solvents, 3:2 T/Ch was identified as the most effective solvent to reduce solid content from 0.66 wt% to 0.49 wt% for DI water and 0.10wt% for HGG at 0.75 vol%, respectively.
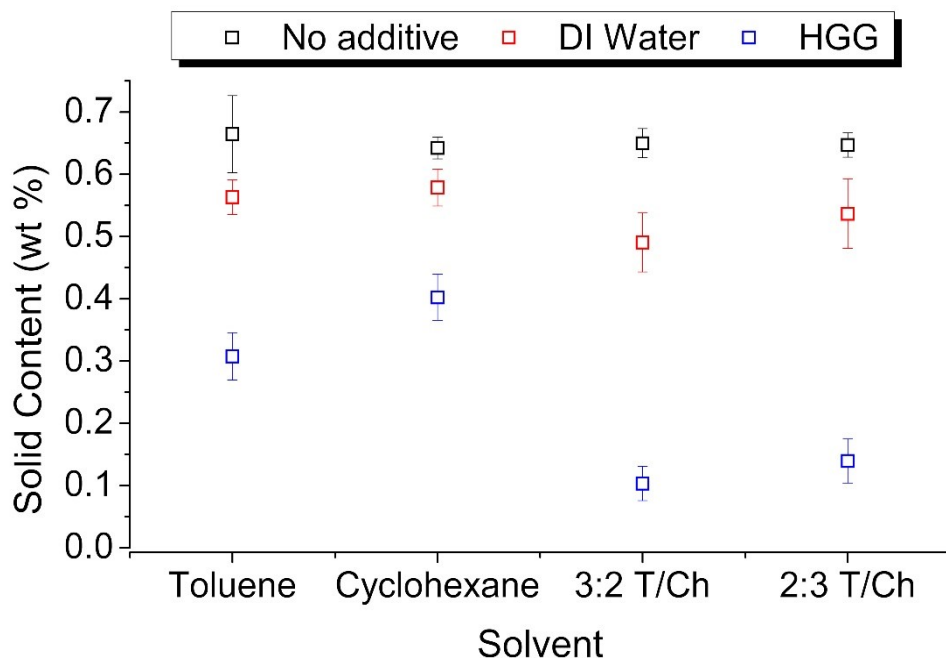
Figure 24 Solid content percentage found in the supernatant after treating with 0.75% Vol of DI water and HGG aqueous in cyclohexane, toluene and their mixtures.

4.2.4.2 Solid content: Effect of HGG concentration

Because of the promising results from HGG, the effect of HGG concentration on the solids content in bitumen was further investigated with same settling procedures and the results are shown in Figure 25. The pure cyclohexane system shows that increasing the concentration of HGG to 1 vol% can decrease the solid content to some extent, however, a further increase of concentration of the HGG could not benefit the decrease of solids content. This phenomenon was

observed in all solvents likely due to the thickening properties of HGG, which, in high quantities, might counteract its flocculant ability. In toluene, an 0.75 vol% HGG is corresponded to lowest solids content.
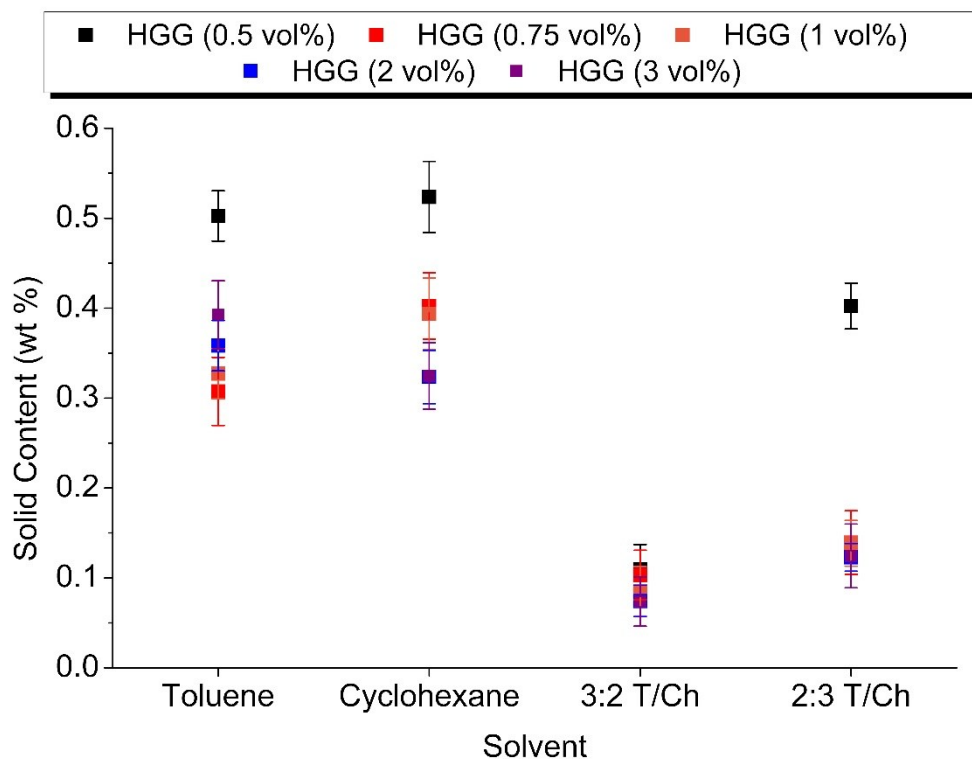
Figure 25 Solid content percentage found in the supernatant after treating with different dosages of HGG aqueous in toluene, cyclohexane and their mixtures.

In mixed solvent systems, results overall improve over pure solvents. In 3:2 T/Ch system at all measured HGG concentrations, the solid content in bitumen was lowest (< 0.1wt%) than other solvents, while an increase of the concentration of HGG does not significantly improve the results. In 2:3 T/Ch system, on the other hand, a significant improvement was observed when the HGG content increased from 0.5 vol% to 0.75 vol%. A general consensus in bitumen product cleaning is to find an efficient additive or chemical aids to aggregate the fine solids for easy

removal, however, the results from our studies demonstrated that the composition of solvent medium plays an equally important role in fine solids removal in bitumen product cleaning. It opens new strategies to deal with the challenging removal of fine solids from bitumen product.

4.3 Analysis of industrial parameters in proposed settling solution

Industrial settings challenge the possible solutions offered by the academia. To make the Non-Aqueous Extraction process feasible to the oil industry the additive proposed must effectively promote aggregation of fine solids in a range of temperatures and at a specific v/v ration between solvent and bitumen. In this section, Ashing and hot filtration protocols were used to determine the total solid content of HGG treated bitumen-solvent systems at different temperatures and with increasing concentration of bitumen to solvent.

4.3.1 Solid content in supernatant: Temperature effect

The procedure of solid content determination used in the previous section was repeated under different temperatures in order to observe the response of our systems to the viscosity of the bitumen-solvent slurry and HGG. Bitumen to solvent ratio was kept at 1:25 and temperature ranging from 17-45°C obtaining results shown in Figure 26.

Several studies have suggested that temperature will affect the viscosity HGG treated systems.[77,78] This behavior is taken into account in our tests, especially because the addition of HGG initially does increase the viscosity of the bitumen diluted in solvent system. We expect that increasing the temperature below the boiling point of the toluene and cyclohexane (~110.8°C and 80.8°C, respectively), we are able to reduce the viscosity of the slurry in order to improve the dispersion of HGG and therefore aggregation for further settling.
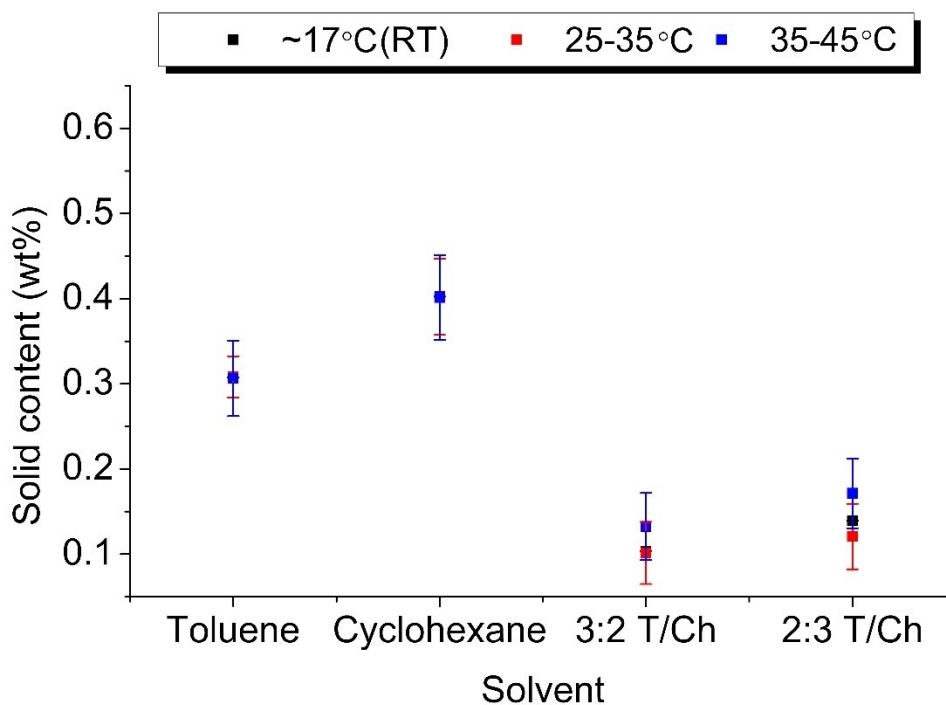
Figure 26 Effect of temperature after treating with 0.75 vol% HGG aqueous in toluene, cyclohexane and their mixtures.

Solid content was in fact affected by the variance in temperatures. A reasonable decrease in solid content is achieved with increasing temperatures from 17-35°C, obtaining a desired improvement and relatively low solid content with temperatures of 25-35°C for the cases of cyclohexane, 3:2 T/Ch and 2:3 T/Ch. However, with increasing temperatures the margin of error also increases. The results in the 35-45°C range highly varied, in some tests the addition of HGG will produce a foam in the slurry while stirring (1100 rpm) at temperatures above 43°C. This behavior only appears at high temperatures; however, it was not present in all the repetitions. Thus, the certainty of the prediction of the effectiveness of the system suggested in this research. Foaming of guar gum has been studied and is due to constant aeration, usually this process is seen in the food industry.[79] However, due to the high stirring rate and lower viscosity, the appearance of foam should not be totally unexpected in our tests.

4.3.2 Solid content in supernatant: Temperature and bitumen to solvent ratio effect

Increasing the ratio of bitumen to solvent is necessary to reduce costs of production. According to industry requirements this ratio should not be higher than 1:5 bitumen to solvent (v/v). The reduction of solvent content was done gradually from the initial mixture ratio up until results were comparable to the initial indigenous bitumen solid content (~0.66 wt%).

With decreasing solvent content, solid content determination presents more difficulty. The slurry formed when bitumen is mixed with each solvent, in addition the introduction of HGG increases the viscosity of the system. The resulting system cannot be easily manipulated and the overall solid content, obtained with the ashing protocol, appears to be the same of the untreated bitumen.

Comparing Figure 26 and Figure 27, an increase in the solid content can be observed independently of the solvent or the temperature, however, mixtures appear to keep the lowest solid content. Increasing the bitumen to solvent ratio proportionally affects the viscosity and therefore the workability of the slurry, thus higher solid content was expected. However, the stirring previous to settling becomes come challenging specially with the introduction of HGG aqueous which increases the viscosity, escalating the difficulty of taking an accurate sample of the supernatant.
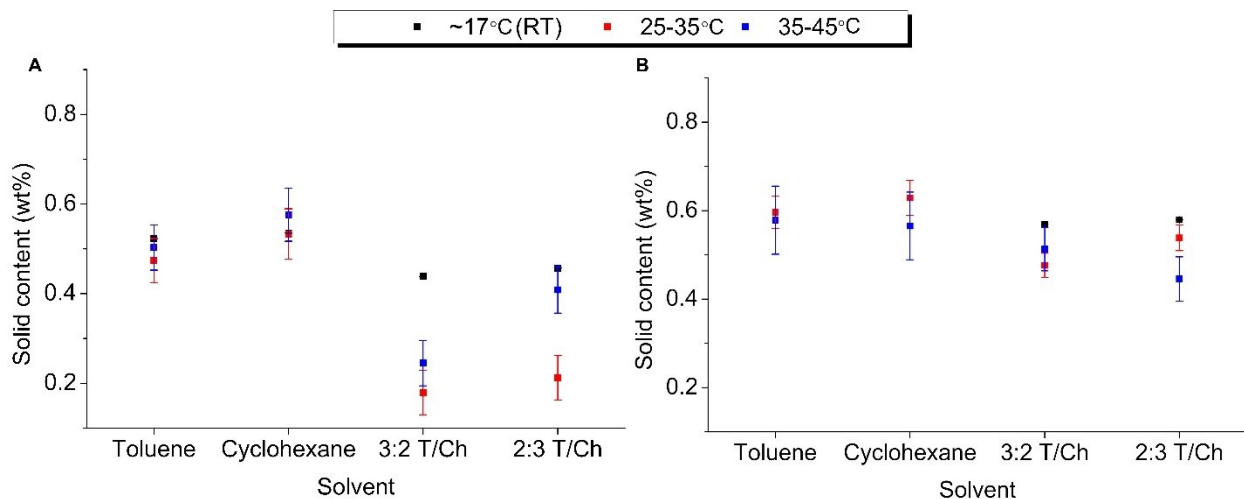
Figure 27 Solid content with 0.75 vol% HGG in toluene, cyclohexane and their mixtures varying temperature at A) 1:15 and B) 1:10 bitumen to solvent ratio.

The ratio of 1:15 bitumen to solvent (Figure 27A), helped us visualize the effect of temperature in highly viscous systems. In pure toluene and cyclohexane, the difference between the solid content results do not have a significant variance, contrary to the results obtained with mixed solvent systems. Under the same temperature conditions, solid content results do not overlap with each other. The 2:3 T/Ch mixture, specially, has a clearly defined range of solid content results for each temperature range.

At a ratio of 1:10 bitumen to solvent (Figure 27B), measurements at room temperature (~17°C) in pure solvent systems were difficult to obtain, results appear to show a higher solid content than the original bitumen sample solid content, therefore, the results do not appear in Figure 27B. The behavior of the systems at this bitumen to solvent ratio is different than the previously analyzed suspensions. The results at high temperatures (35-45°C) do, in fact, show that increasing the temperature enhances the effect of the proposed aggregation system. However, desired solid content was not achieved. An increment in vol% of HGG aqueous was

proposed, nonetheless, this addition will increase the viscosity of the system, complicating the testing process.

CHAPTER 5   SUMMARY AND FUTURE WORK

In order to meet the specifications of pipeline transport and refinery feed, destabilizing the fine solids in organic media must be done in order to remove fine solids from bitumen obtained by non-aqueous extraction (NAE) of Alberta oil sands. Destabilizing the fine solids in organic media is the first step for the effective removal of fine solids from bitumen product. This research showed promising progress towards applying surface active chemicals with desired functional groups to modify the interfacial chemistry of fine solids and oil/water interfaces of water drops to further to develop an effective method to decrease the content of fine solids in NAE bitumen. Two settling processes were investigated: a model in which DI water, LGG and HGG were used as aids in the settling bitumen-coated silica particles in toluene; and DI water and HGG- assisted settling of indigenous fine solids in diluted bitumen.

In the first part of this work we demonstrated a way to destabilize the bitumen-coated silica particles in toluene through addition of water-assisted biomolecules extracted from the natural guar bean. Two kinds of well-known extracted guar gum, a low molecular weight disodium[[[5-(6-aminopurin-9-yl)-3-hydroxyoxolan-2-yl]methoxy-hydroxyphosphoryl]oxy-oxidophosphoryl] hydrogen phosphate (LGG) and a high molecular weight polysaccharide (HGG), were examined. It is observed that the performance in fast settling and in lowering solid content of guar gum to destabilize the bitumen-coated silica particles followed the order: water only < LGG only < LGG aqueous solution < HGG aqueous solution ≈ HGG only. The LGG, an amphiphilic chemical, could facilitate the aggregation of bitumen-coated silica particles by modifying the surface of the solids, rendering the solid particles less oleophilic and more hydrophilic. The modification by LGG could be further facilitated by adding water to LGG to the system because the added water provided water/oil interfaces to stabilize and disperse the LGG,

significantly increasing the effectiveness of interaction between the gum and solid particles. Simultaneously, the presence of water could trigger the formation of agglomerates with the modified solid particles and remarkably accelerate the settling process. Different from LGG, the HGG acted as a flocculant to destabilize the bitumen-coated silica particles by means of forming large solid flocs which readily settled out by gravitational force. Due to the robust effects of flocculation by HGG, the introduction of water did not improve the settling performance.

In addition, this work demonstrated a way to improve fine solids settling for further removal by modifying the aromatic character of the solvent when DI water and HGG aqueous assisted settling in bitumen-diluted systems. Toluene, cyclohexane and their mixtures in 3:2 and 2:3 toluene/cyclohexane volume ratio, where the solvents used to study the aromaticity effect in the settling of fine solids. Focus beam reflectance measurements (FBRM) showed that DI water droplets have distinct size distributions according to the solvent. Smaller and stable water droplets (water-in-oil emulsion) appear at constant stirring speed in toluene. Overall, water droplets have smaller chord lengths than HGG aggregates regardless of the solvent. However, in bitumen-diluted systems the sizes of the aggregates formed by the addition of DI water have high counts in chord lengths between 21-60µm, before settling. In terms of solid content of the supernatant after settling, HGG significantly reduces the solid content independently of the aromaticity of the solvent. Solvent mixtures substantially reduce the solid content, specifically if the content of the aromatic solvent surpasses the one of the aliphatic or non-aromatic. A solid content reduction of ~80% at 3:2 toluene/cyclohexane was observed.

The effect of temperature under a visco-elastic range (17-45°C) and solvent concentration in bitumen-diluted systems were also studied in order to analyze the influence of viscosity in HGG aqueous-assisted settling. Results showed promising results for high temperatures,

however, due to the added viscosity inherent of HGG, the higher temperatures in the visco-elastic range are not enough to provide a solution for effective settling at low solvent content bitumen diluted slurry.

A continuation of this work must be done to address these challenges in order to stablish an effective method to complement NAE and increase its feasibility. Future work must focus on twos aspects: To investigate the interaction mechanism among guar gum, fine solids and water drops in the complex organic media using techniques such as QCM-D measurements, atomic force measurements (AFM) and contact angle. And to further investigate the effect of industrial settings.

The effect of industrial settings must be further studied. This study only provided insight information on the effect temperatures in the visco-elastic range. Additional equipment and techniques must be employed to increase temperature uniformly throughout mixing and settling process to be analyzed. In addition, the process used in this research specified mixing techniques and velocities that might not converge with the industrial capacity or technology (e.g sonication and stirring at 1100 rpm). Therefore, the effects of the mechanical stirring rate and sonication in removing the fine solids from indigenous bitumen must, also, be studied.

The results provided insights into the development of methods that can complement the extraction of bitumen itself. Although non-aqueous extraction has not been an economically and resource viable method for bitumen extraction, this research is a good directive to improve the feasibility of NAE conductive to an environmentally friendly fossil fuel extraction.

REFERENCES

(1)   Alberta Government. *Energy Annual Report 2017-2018*; 2018.

(2)   J Masliyah, J Czarnecki, Z. X. *Handbook on Theory and Practice of Bitumen Recovery from Athabasca Oil Sands, Volume 1: Theoretical Basis*; Canada: Kingsley Knowledge Publishing, 2011.

(3)   Speight, J. G. A Review of: "The Chemistry of Alberta Oil Sands Bitumens and Heavy Oils." *Energy Sources* **2005**, *27* (8), 780–780.

(4)   (CAPP), C. A. of P. P. Oil Extraction. Oil Sands Recovery https://www.capp.ca/oil/extraction/.

(5)   OIL SANDS MAGAZINE. MINING VERSUS IN-SITU: A LOOK AT HOW ENERGY COMPANIES ARE SHIFTING THEIR PRIORITIES https://www.oilsandsmagazine.com/news/2016/7/18/mining-versus-in-situ-how-energy-companies-are-shifting-their-priorities.

(6)   Osacky, M.; Geramian, M.; Ivey, D. G.; Liu, Q.; Etsell, T. H. Influence of Nonswelling Clay Minerals (Illite, Kaolinite, and Chlorite) on Nonaqueous Solvent Extraction of Bitumen. *Energy and Fuels* **2015**, *29* (7), 4150–4159.

(7)   Hooshiar, A.; Uhlik, P.; Liu, Q.; Etsell, T. H.; Ivey, D. G. Clay Minerals in Nonaqueous Extraction of Bitumen from Alberta Oil Sands: Part 1. Nonaqueous Extraction Procedure. *Fuel Processing Technology* **2012**, *94* (1), 80–85.

(8)   Xu, Y.; Dabros, T.; Hamza, H. Study on the Mechanism of Foaming from Bitumen Froth Treatment Tailings. *Journal of Dispersion Science and Technology* **2007**, *28* (3), 413–418.

(9)   Pal, K.; Nogueira Branco, L. D. P.; Heintz, A.; Choi, P.; Liu, Q.; Seidl, P. R.; Gray, M. R. Performance of Solvent Mixtures for Non-Aqueous Extraction of Alberta Oil Sands. *Energy and Fuels* **2015**, *29* (4), 2261–2267.

(10)   Buenrostro-gonzalez, E.; Groenzin, H.; Lira-galeana, C.; Mullins, O. C. Asphaltenes. **2001**, No. 13, 972–978.

(11)   Zhang, L. Y.; Breen, P.; Zhenghe, X.; Masliyah, J. H. Asphaltene Films at a Toluene/Water Interface. *Energy Fuels* **2007**, *21* (1), 274–285.

(12)   Fossen, M.; Kallevik, H.; Knudsen, K. D.; Sjöblom, J. Asphaltenes Precipitated by a Two-Step Precipitation Procedure. 1. Interfacial Tension and Solvent Properties. *Energy Fuels* **2007**, *21* (2), 1030–1037.

(13)   Osacký, M.; Geramian, M.; Uhlík, P.; Čaplovičová, M.; Danková, Z.; Pálková, H.; Vítková, M.; Kováčová, M.; Ivey, D. G.; Liu, Q.; et al. Mineralogy and Surface Chemistry of Alberta Oil Sands: Relevance to Nonaqueous Solvent Bitumen Extraction. *Energy and Fuels* **2017**, *31* (9), 8910–8924.

(14)   Sparks, B. D.; Meadus, F. W. A Study of Some Factors Affecting Solvent Losses in the Solvent Extraction — Spherical Agglomeration of Oil Sands. *Fuel Processing Technology* **1981**, *4*, 251–264.

(15)   Sparks, B. D.; Meadus, F. W.; Hoefele, E. O. Solvent Extraction Spherical Agglomeration of Oil Sands. *United States Patent* **1988**, 1–23.

(16)   Tan, X.; Fenniri, H.; Gray, M. R. Water Enhances the Aggregation of Model Asphaltenes in Solution via Hydrogen Bonding. *Energy & Fuels* **2009**, *23* (15), 9080–9086.

(17)   Yan, N.; Gray, M. R.; Masliyah, J. H. On Water-in-Oil Emulsions Stabilized by Fine Solids. *Colloids and Surfaces* **2001**, *193*, 97–107.

(18)   Gorski, J.; Lothian, N.; Severson-Baker, C.; Way, N. *The Oilsands in a Carbon-Constrained Canada The Collision Course between Overall Emissions and National Climate Commitments Benjamin Israel*; 2020.

(19)   Li, D. D.; Greenfield, M. L. Chemical Compositions of Improved Model Asphalt Systems for Molecular Simulations. *Fuel* **2014**, *115*, 347–356.

(20)   D'Melo, D.; Taylor, R. Constitution and Structure of Bitumens. *The Shell Bitumen Handbook* **2015**, 47–62.

(21)   Laukkanen, O. V.; Soenen, H.; Winter, H. H.; Seppälä, J. Low-Temperature Rheological and Morphological Characterization of SBS Modified Bitumen. *Construction and Building Materials* **2018**, *179*, 348–359.

(22)   Van Poel, C. Der. A General System Describing the Visco-Elastic Properties of Bitumens and Its Relation to Routine Test Data. *Journal of Applied Chemistry* **2007**, *4* (5), 221–236.

(23)   Oliviero Rossi, C.; Spadafora, A.; Teltayev, B.; Izmailova, G.; Amerbayev, Y.; Bortolotti, V. Polymer Modified Bitumen: Rheological Properties and Structural Characterization. *Colloids and Surfaces A: Physicochemical and Engineering Aspects* **2015**, *480*, 390–397.

(24)   Speight, J. G. Asphaltenes and the Structure of Petroleum. *Oil and Gas Science and Technology* **1998**, *59* (5), 467–477.

(25)   Speight, J. G. Latest Thoughts on the Molecular Nature of Petroleum Asphaltenes. *Preprints Symposia* **1989**, *34* (2), 321–328.

(26)   Speight, J. G. Asphaltenes in Crude Oil and Bitumen: Structure and Dispersion. *Advances in Chemistry Series* **1996**, *251*, 397–401.

(27)   Speight, J. G. Asphaltenes: Fundamentals and Applications By E. Y. Sheu and O. C. Mullins. Plenum Press, New York, 1995; 236 Pages plus Index. $79.50. ISBN No. 0-306-45191-3. *Energy & Fuels* **1996**, *10* (6), 1282–1282.

(28)   Gutierrez, L.; Pawlik, M. Influence of Humic Acids on Oil Sand Processing. Part I: Detection and Quantification of Humic Acids in Oil Sand Ores and Their Effect on Bitumen Wettability. *International Journal of Mineral Processing* **2014**, *126*, 117–125.

(29)   Sparks, B. D.; Kotlyar, L. S.; O'Carroll, J. B.; Chung, K. H. Athabasca Oil Sands: Effect of Organic Coated Solids on Bitumen Recovery and Quality. *Journal of Petroleum Science and Engineering* **2003**, *39* (3–4), 417–430.

(30)   Chen, Q.; Liu, Q. Bitumen Coating on Oil Sands Clay Minerals: A Review. *Energy and Fuels* **2019**, *33* (7), 5933–5943.

(31)   Liu, J.; Wang, J.; Huang, J.; Cui, X.; Tan, X.; Liu, Q.; Zeng, H. Heterogeneous Distribution of Adsorbed Bitumen on Fine Solids from Solvent-Based Extraction of Oil Sands Probed by AFM. *Energy & Fuels* **2017**, *31* (9), 8833–8842.

(32)   Anderson, W. G. Wettability Literature Survey - Part 1: Rock-Oil-Brine Interactions and the Effects of Core Handlding on Wettability. *Society of Petroleum Engineers of AIME, (Paper) SPE* **1985**, No. October, 1125–1144.

(33)   Hall, A. C.; Collins, S. H.; Melrose, J. C. Stability of Aqueous Wetting Films in Athabasca Tar Sands. *Society of Petroleum Engineers journal* **1983**, *23* (2), 249–258.

(34)   Srinivasa, S. Study of Bitumen Liberation from Oil Sands Ores. Master Thesis. **2010**, 96.

(35)   Takamura, K. Microscopic Structure of Athabasca Oil Sand. *The Canadian Journal of Chemical Engineering* **1982**, *60* (4), 538–545.

(36)   Gray, M. R.; Tykwinski, R. R.; Stryker, J. M.; Tan, X. Supramolecular Assembly Model for Aggregation of Petroleum Asphaltenes. *Energy and Fuels* **2011**, *25* (7), 3125–3134.

(37)   Majid, A.; Ripmeester, J. A. Characterization of Unextractable Organic Matter Associated with Heavy Metal Minerals from Oil Sand. *Preprints Symposia* **1986**, *31* (2), 634.

(38)   Ren, S.; Zhao, H.; Dang-Vu, T.; Xu, Z.; Masliyah, J. H. Effect of Weathering on Oil Sands Processability. *Canadian Journal of Chemical Engineering* **2009**, *87* (6), 879–886.

(39)   Couillard, M.; Mercier, P. H. J. Analytical Electron Microscopy of Carbon-Rich Mineral Aggregates in Solvent-Diluted Bitumen Products from Mined Alberta Oil Sands. *Energy and Fuels* **2016**, *30* (7), 5513–5524.

(40)   Chen, Q.; Stricek, I.; Gray, M. R.; Liu, Q. Influence of Hydrophobicity Distribution of Particle Mixtures on Emulsion Stabilization. *Journal of Colloid and Interface Science* **2017**, *491*, 179–189.

(41)   Wu, J.; Dabros, T. Process for Solvent Extraction of Bitumen from Oil Sand. *Energy and Fuels* **2012**, *26* (2), 1002–1008.

(42)   Liu, J.; Xu, Z.; Masliyah, J. Interaction between Bitumen and Fines in Oil Sands Extraction System: Implication to Bitumen Recovery. *The Canadian Journal of Chemical Engineering* **2008**, *82* (4), 655–666.

(43)   Lin, F.; Stoyanov, S. R.; Xu, Y. Recent Advances in Nonaqueous Extraction of Bitumen

from Mineable Oil Sands: A Review. *Organic Process Research and Development*. 2017.

(44)   Wang, T.; Zhang, C.; Zhao, R.; Zhu, C.; Yang, C.; Liu, C. Solvent Extraction of Bitumen from Oil Sands. *Energy and Fuels* **2014**, *28* (4), 2297–2304.

(45)   Tian, Y.; McGill, W. B.; Whitcombe, T. W.; Li, J. Ionic Liquid-Enhanced Solvent Extraction for Oil Recovery from Oily Sludge. *Energy and Fuels* **2019**, *33* (4), 3429–3438.

(46)   Tan, X.; Fenniri, H.; Gray, M. R. Water Enhances the Aggregation of Model Asphaltenes in Solution via Hydrogen Bonding. *Energy and Fuels* **2009**, *23* (7), 3687–3693.

(47)   Thombare, N.; Jha, U.; Mishra, S.; Siddiqui, M. Z. International Journal of Biological Macromolecules Guar Gum as a Promising Starting Material for Diverse Applications : A Review. *International Journal of Biological Macromolecules* **2016**, *88*, 361–372.

(48)   Yousif, M. E.; Mohamed, B. E.; AE, E. Physicochemical Characterization of Gum of Some Guar (Cyamposis Tetragonoloba L. Taup) Lines. *Journal of Food Processing & Technology* **2017**, *08* (02), 8–11.

(49)   Hasan, A. M. A.; Abdel-Raouf, M. E. Applications of Guar Gum and Its Derivatives in Petroleum Industry: A Review. *Egyptian Journal of Petroleum* **2018**, *27* (4), 1043–1050.

(50)   Gupta, B. Sen; Ako, J. E. Application of Guar Gum as a Flocculant Aid in Food Processing and Potable Water Treatment. *European Food Research and Technology* **2005**, *221* (6), 746–751.

(51)   Pal, S.; Mal, D.; Singh, R. P. Synthesis and Characterization of Cationic Guar Gum: A High Performance Flocculating Agent. *Journal of Applied Polymer Science* **2007**, *105* (6),

3240–3245.

(52)   Singh, R. P.; Karmakar, G. P.; Rath, S. K.; Karmakar, N. C.; Pandey, S. R.; Tripathy, T.; Panda, J.; Kanan, K.; Jain, S. K.; Lan, N. T. Biodegradable Drag Reducing Agents and Flocculants Based on Polysaccharides: Materials and Applications. *Polymer Engineering & Science* **2000**, *40* (1), 46–60.

(53)   Database, C. Guar gum-9000-30-0 https://www.chemicalbook.com/ProductChemicalPropertiesCB5253559_EN.htm (accessed Jan 7, 2018).

(54)   Li, Z.; Lu, P.; Zhang, D.; Chen, G.; Zeng, S.; He, Q. Population Balance Modeling of Activated Sludge Flocculation: Investigating the Influence of Extracellular Polymeric Substances (EPS) Content and Zeta Potential on Flocculation Dynamics. *Separation and Purification Technology* **2016**, *162*, 91–100.

(55)   Urbina-Villalba, G.; Toro-Mendoza, J.; Lozsán, A.; García-Sucre, M. Effect of the Volume Fraction on the Average Flocculation Rate. *Journal of Physical Chemistry B* **2004**, *108* (17), 5416–5423.

(56)   Vajihinejad, V.; Soares, J. B. P. Monitoring Polymer Flocculation in Oil Sands Tailings: A Population Balance Model Approach. *Chemical Engineering Journal* **2018**, *346* (April), 447–457.

(57)   Carissimi, E.; Rubio, J. Polymer-Bridging Flocculation Performance Using Turbulent Pipe Flow. *Minerals Engineering* **2015**, *70*, 20–25.

(58)   Ghorai, S.; Sarkar, A.; Panda, A. B.; Pal, S. Evaluation of the Flocculation Characteristics

of Polyacrylamide Grafted Xanthan Gum/Silica Hybrid Nanocomposite. *Industrial and Engineering Chemistry Research* **2013**, *52* (29), 9731–9740.

(59) Butt, H.-J.; Graf, K.; Kappl, M. *Physics and Chemistry of Interfaces*; WILEY-VCH GmbH & Co., 2006.

(60) Israelachvili, J. N. *Intermolecular and Surface Forces*; Reserved, C. © 2011 E. I. A. rights, Ed.; ACADEMIC PRESS, INC., 2011.

(61) Park, J. M.; Kwon, D. J.; Wang, Z. J.; Byun, J. H.; Lee, H. I.; Park, J. K.; DeVries, L. K. Novel Method of Electrical Resistance Measurement in Structural Composite Materials for Interfacial and Dispersion Evaluation with Nano- And Hetero-Structures. *Materials Research Society Symposium Proceedings* **2014**, *1700*, 37–46.

(62) Lu, Q.; Huang, J.; Liu, Y.; Zeng, H.; Yan, B.; Xie, L. A Two-Step Flocculation Process on Oil Sands Tailings Treatment Using Oppositely Charged Polymer Flocculants. *Science of The Total Environment* **2016**, *565*, 369–375.

(63) International Petroleum Test methods. Standard Test Method for Ash from Petroleum Products. D482 − 19, 2008.

(64) American Petroleum institute. Standard Test Method for Sediment in Crude Oil by Membrane Filtration. D4807 − 05, 2015.

(65) Autochem, M. Particle Characterization Track Particles in Real Time Optimize and Monitor Processes. Mettler-Toledo AutoChem, Inc. 2006.

(66) Liu, J.; Cui, X.; Huang, J.; Xie, L.; Tan, X.; Liu, Q.; Zeng, H. Understanding the Stabilization Mechanism of Bitumen-Coated Fine Solids in Organic Media from Non-

Aqueous Extraction of Oil Sands. *Fuel* **2019**, *242* (January), 255–264.

(67) Tadayyon, A.; Rohani, S. Determination of Particle Size Distribution by Par-Tec® 100: Modeling and Experimental Results. *Particle and Particle Systems Characterization* **1998**, *15* (3), 127–135.

(68) Liu, J.; Cui, X.; Santander, C.; Tan, X.; Liu, Q.; Zeng, H. Destabilization of Fi Ne Solids Suspended in Oil Media through Wettability Modi Fi Cation and Water-Assisted Agglomeration. *Fuel* **2019**, *254* (March), 115623.

(69) Natarajan, A.; Xie, J.; Wang, S.; Masliyah, J.; Zeng, H.; Xu, Z. Understanding Molecular Interactions of Asphaltenes in Organic Solvents Using a Surface Force Apparatus. *The Journal of Physical Chemistry C* **2011**, *115* (32), 16043–16051.

(70) Natarajan, A.; Kuznicki, N.; Harbottle, D.; Masliyah, J.; Zeng, H.; Xu, Z. Understanding Mechanisms of Asphaltene Adsorption from Organic Solvent on Mica. *Langmuir* **2014**, *30* (31), 9370–9377.

(71) Zhang, L.; Shi, C.; Lu, Q.; Liu, Q.; Zeng, H. Probing Molecular Interactions of Asphaltenes in Heptol Using a Surface Forces Apparatus : Implications on Stability of Water-in-Oil Emulsions. *Langmuir* **2016**, No. 32, 4886−4895.

(72) Mahmoud, N. M. Physico-Chemical Study on Guar Gum. MSc Thesis, Department of Chemistry, University of Khartoum, 2000.

(73) Towle, G. A.; Whistler, R. L. *Chemical Modification of Gums*; 2012. (74) Tan, X.; Reed, A. H.; Hu, L.; Zhang, G.; Furukawa, Y. Flocculation and Particle Size Analysis of Expansive Clay Sediments Affected by Biological, Chemical, and Hydrodynamic Factors.

Ocean Dynamics **2013**, *64* (1), 143–157.

(75)   Jayawardena, B.; Pantithavidana, D.; Sameera, W. Polysaccharides in Solution: Experimental and Computational Studies. *Intech open* **2015**, *2*, 64.

(76)   Garcia Vidal, C. A.; Pawlik, M. Molecular Weight Effects in Interactions of Guar Gum with Talc. *International Journal of Mineral Processing* **2015**, *138*, 38–43.

(77)   Kulkarni, A. R.; Soppimath, K. S.; Aminabhavi, T. M. Rheological Properties of the Dispersions of Starch, Guar Gum, and Their Physical Mixtures in the Temperature Interval 298.15-333.15 K. *Polymer - Plastics Technology and Engineering* **2000**, *39* (3), 437–456.

(78)   Wang, S.; He, L.; Guo, J.; Zhao, J.; Tang, H. Intrinsic Viscosity and Rheological Properties of Natural and Substituted Guar Gums in Seawater. *International Journal of Biological Macromolecules* **2015**, *76*, 262–268.

(79)   Kabziński, M.; Neupauer, K.; Nowak, M.; Kruk, J.; Kaczmarczyk, K. The Impact of Addition of Xanthan Gum and Guar Gum on Rheological Properties of Foams Produced by Continuous Method. *Polimery/Polymers* **2019**, *64* (7–8), 538–541.

(80)   Jin, Y.; Liu, W.; Liu, Q.; Yeung, A. Aggregation of Silica Particles in Non-Aqueous Media. *Fuel* **2011**, *90* (8), 2592–2597.

Appendix A: FBRM measurement of bare silica and bitumen coated silica particles.

For the size measurement of bare silica and bitumen coated silica particles, the FBRM probe was immersed into a 250 mL beaker containing pure toluene and 1 gram of solids (bare and coated silica) were added with constant stirring rate of 1100 rpm. The scanning laser was focused to a fine spot at the sapphire window interface and this optical signal was then processed.
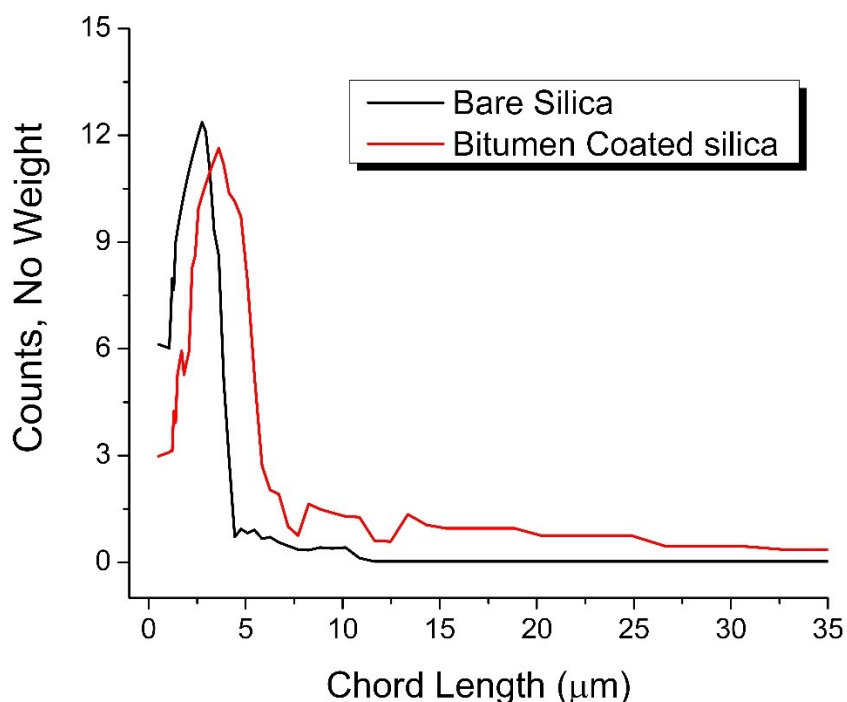
Figure A. FBRM measurement of bare and coated silica in toluene.

For bare silica, the average size of the particles is observed around ~2.6 μm, with a steep slope following. In bitumen coated silica, it was noticed a peak around ~4.3 μm. In both cases

there are several counts on a larger scale (~10 µm), due to the formation of aggregates cause by the disturbed system.

Appendix B: FBRM of bitumen coated silica particles vs LGG and HGG

The FBRM probe was immersed into a 250 mL beaker containing pure toluene and Bitumen-coated silica particles, LGG and HGG were individually added at 1.5 wt% and at constant stirring rate of 1100 rpm. The scanning laser was focused to a fine spot at the sapphire window interface and this optical signal was then processed.
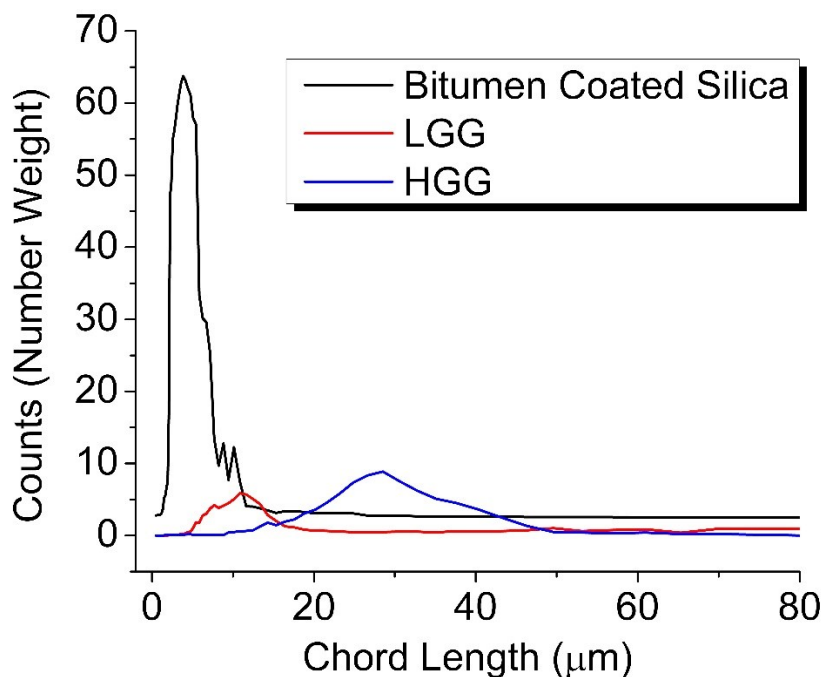
Figure B. FBRM measurement comparison between the prepared bitumen coated silica, LGG and HGG at 1.5 wt% in toluene.

In bitumen coated silica, it was noticed a peak around ~4.3 µm, with several count over 60 number weight. For LGG and HGG, the peaks were found ~11 µm and ~27 µm, respectively. Counts from both gums do not surpass ~ 10 number weight. The same process was done from 1-

3 vol% and in all cases the gums percentage of counts did not increase above 10% in relation to the number of coated particles.

Appendix C: LGG and HGG settling curve.

LGG and HGG, separately, were mixed with toluene at ~ 0.5 vol% additive. The mixture was sonicated for 5 min and agitated using a magnetic stirrer (1100 rpm) for 10 min. Then, the mixture is transferred to a 100 mL graduated cylinder. During the sedimentation process, the changes of mudline location in the cylinder (mL) were recorded as a function of settling time (s). The dosage of the additives was expresses based on the amount of toluene.
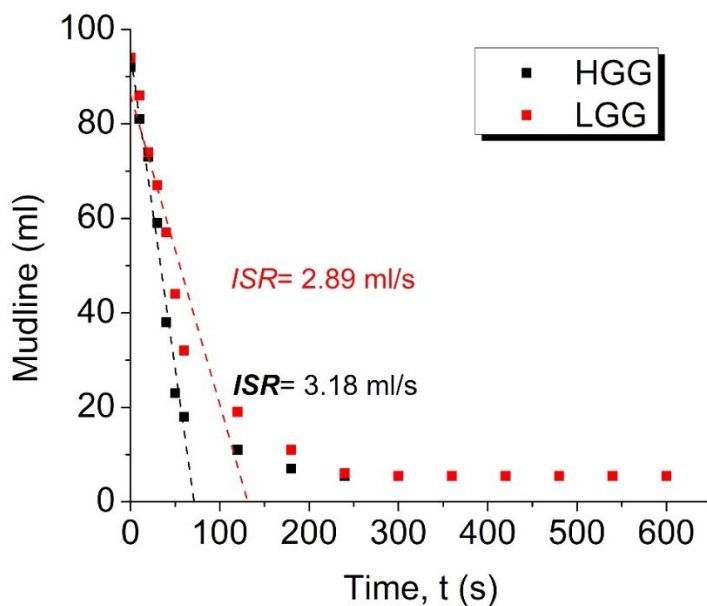
Figure C. Settling results of the LGG (red squares) and the HGG (black squares) in toluene.

The settling curve clearly shows that both LGG and HGG additives have a high settling rate. However, HGG presents a higher settling rate that can be attributed to its molecular weight and its hydrophilic nature.

Appendix D: FBRM measurement of pure LGG and HGG in Toluene.

To measure the size of Guar gum aggregates without fine solids, both gums were diluted in toluene at ~90 wt% gum. The FBRM probe was immersed into a 250 mL beaker containing pure toluene and the LGG and HGG (90 wt%) dilutions were added with constant stirring rate of 1100 rpm. The concentration of both diluted Guar gums was increased from 0.5 to 3 %Vol. The scanning laser was focused to a fine spot at the sapphire window interface and this optical signal was then processed.
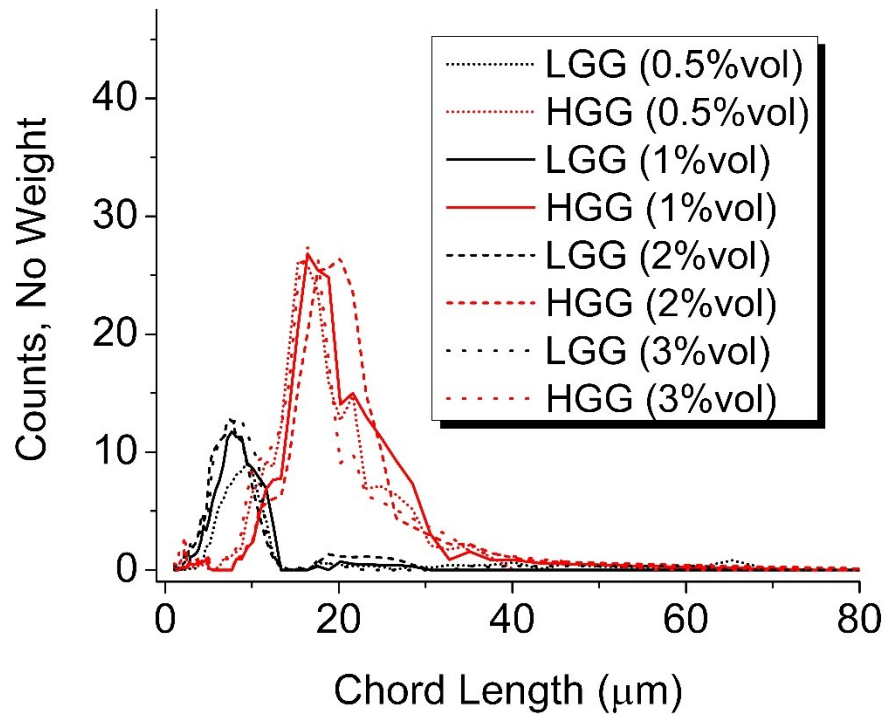
Figure D. FBRM measurement of different concentrations of pure LGG and HGG in Toluene.

For LGG, the average size, independent of the concentration, can be found in ~8μm. However, concentration does affect the counts, increasing them accordingly. In the HGG case it was noticed that the peaks have a slight shift depending on the concentration, nonetheless, the average size is found between 15-25μm. The difference between the size is expected dictated by

the molecular weight of both gums. However, HGG tends to aggregate more, which is confirmed with the shift in size instead of the increase in counts.

Appendix E: Settling curve of HGG in organic solvents

HGG was introduced toluene, cyclohexane, and toluene/cyclohexane mixtures (3:2 and 2:3 T/Ch volume ratio). The suspension was stirred at 1100 rpm for 1 min and transferred to a 100 mL graduated cylinder. The changes of mudline location in the cylinder (mL) were recorded as a function of settling time (s) as shown in Figure S1.
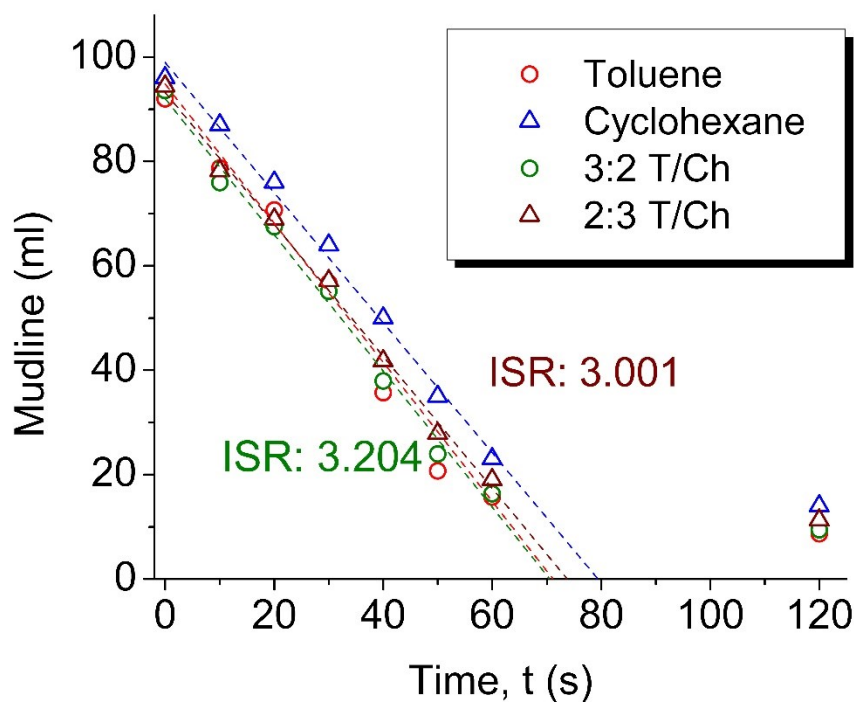
Figure E Settling curves of HGG in toluene, cyclohexane, 3:2 T/Ch and 2:3 T/Ch. Initial settling rates of 3:2 T/Ch (green insert) and 2:3 T/Ch (wine insert).

Settling rates of HGG in toluene, cyclohexane and their mixture show no significant difference. However, the results show that the settling rates in mixtures are closer the settling rate of toluene. The slight differences between them could be due to human error.

Appendix F: Initial fine solid counts

A 1:25 vol. bitumen/solvent was prepared, sonicated for 5 min and agitated using a magnetic stirrer (1100 rpm) for an additional 10 min. The bitumen-solvent solutions were transferred to 250 mL beaker, maintaining the stirring rate. The scanning laser was focused to a fine spot at the sapphire window interface and this optical signal was then processed. The total number of aggregates (No Weight) before any addition of DI water or HGG was obtained.

Table A Total counts and according to size counts of fine solids aggregates before the addition of water and HGG in the bitumen-solvent solutions.

	Total counts (No Weight)			
	Before settling			
	Chord length (µm)			Total
Solvent	1-10	11-20	21-60	
Toluene	$1983 \pm 1.5\%$	$272 \pm 6.0\%$	$5 \pm 4.0\%$	$2260 \pm 2.5\%$
Cyclohexane	$1580 \pm 2.7\%$	$444 \pm 2.7\%$	$59 \pm 3.0\%$	$2083 \pm 3.5\%$
3:2 T/Ch	$1789 \pm 1.5\%$	$313 \pm 3.5\%$	$26 \pm 3.4\%$	$2128 \pm 2.7\%$
2:3 T/Ch	$1617 \pm 2.2\%$	$426 \pm 2.1\%$	$32 \pm 4.3\%$	$2075 \pm 2.8\%$

Overall, the total number of fine solids in the bitumen samples used in the settling tests with different solvents $2164 \pm 6.1\%$. The number of fine solids aggregates varies slightly independently of the solvent used. High number of counts in the lower range (1-10 µm) was found in all solvents, however, a clear difference can be seen between the number of fine solids or small aggregates toluene and 3:2 T/Ch, and cyclohexane and 2:3 T/Ch. In addition, we found that there is a larger number of aggregates in the upper ranges (11-60 µm) is found in the solvents with high cyclohexane; with higher content of cyclohexane, the aromatic character of

the solvent decreases conducing to fine solid aggregation.[80] Regardless, the total counts of

aggregates are attributed to the initial fine solid content in each sample.